PPD 0 and returned to the virgin control level at PPD 28 (on weaning), indicating that this biological control mechanism may also be present during lactation. Experiments remain to be performed on whether prolactin and/or oxytocin could suppress the activities of drug metabolizing enzymes and reduce CYPs protein.

Oxidative stress may be one of the factors which are responsible for the regulation of CYPs during rat lactation. Oxidative stress has been suggested to result in the reduction of total CYP450 levels and drug metabolizing activities in vivo (Mannering and Deloria, 1986; Peristeris et al., 1992; Gatti et al., 1993; Liu et al., 1993). Furthermore, Barker et al. (1994) have investigated the possibility that oxidative stress may influence inducer-dependent expression of CYP1A1 and CYP1A2 and demonstrated that hydrogen peroxide suppresses the accumulation of CYP1A1 and CYP1A2 mRNAs in isolated hepatocytes through a transcriptional mechanism. Pahan et al. (1997) demonstrated that there is a down-regulation of CYP2E1 in rat liver peroxisomes by a mechanism of ischemia/reperfusion-induced oxidative stress. Investigation by Upreti et al. (2002) indicated that significantly higher lipid peroxidation levels were established in all the major organs of rat during lactation. Furthermore, they also demonstrated that the early lactation generated higher oxidative stress compared with the late periods of lactation. This seems to be consistent with our data: six CYPs proteins were markedly decreased at PPD 0, and four of them returned to the virgin control level on PPD 14. In human, lipid peroxidation is increased during pregnancy, and delivery alone is a major source of oxidative stress (Arikan et al., 2001), probably confirming the results obtained at PPD 0 in this study. Therefore, oxidative stress may play a role in the regulation of CYPs protein during rat lactation.

Although endogenous nitric oxide (NO), a potent vasodilator and a platelet anti-aggregating factor, has been suggested to be involved in the regulation of CYPs protein during rat pregnancy (He et al., 2005), the data of changes in NO during rat lactation are absent.

Taken together, the results of the present study suggest that rat lactation is accompanied with decreases in some CYPs proteins levels. Effects of lactation on decreases in CYPs protein levels were more predominant at birth day (PPD 0) than at peak lactation (PPD 14). All the decreased CYPs proteins were at virgin control levels by 7 days post-lactation (PPD 28), clearly suggesting that biological changes during rat lactation could influence the expression of hepatic CYPs protein. Further studies are required to elucidate the mechanism of effects of lactation on down-regulation of CYPs protein.

References

Abel, E.L., Greizerstein, H.B., Siemens, A.J., 1979. Influence of lactation on rate of disappearance of ethanol in the rat. Neurobehav. Toxicol. 1, 185–186.

Arikan, S., Konukoglu, D., Arikan, C., Akcay, T., Davas, I., 2001. Lipid peroxidation and antioxidant status in maternal and cord blood. Gynecol. Obstet. Invest. 51, 145–149.

Barker, C.W., Fagan, J.B., Pasco, D.S., 1994. Down-regulation of P4501A1 and P4501A2 mRNA expression in isolated hepatocytes by oxidative stress. J. Biol. Chem. 269, 3985–3990.

Borlakoglu, J.T., Scott, A., Henderson, C.J., Wolf, C.R., 1993. Alterations in rat hepatic drug metabolism during pregnancy and lactation. Biochem. Pharmacol. 46, 29–36.

Dean, M.E., Stock, B.H., 1975. Hepatic microsomal metabolism of drugs during pregnancy in the rat. Drug Metab. Dispos. 3, 325–331.

Dean, M.E., Stock, B.H., 1989. The influence of phenobarbital administration on hepatic monooxygenase activity at various stages of gestation in the rat. Drug Metab. Dispos. 17, 579–581.

Feuer, G., 1979. Action of pregnancy and various progesterones on hepatic microsomal activities. Drug Metab. Rev. 9, 147–169.

Feuer, G., Liscio, A., 1969. Origin of delayed development of drug metabolism in the newborn rat. Nature 223, 68–70.

Gatti, S., Faggioni, R., Echtenacher, B., Ghezzi, P., 1993. Role of tumour necrosis factor and reactive oxygen intermediates in lipopolysaccharide-induced pulmonary oedema and lethality. Clin. Exp. Immunol. 91, 456–461.

Guarino, A.M., Gram, T.E., Schroeder, D.H., Call, J.B., Gillette, J.R., 1969. Alterations in kinetic constants for hepatic microsomal aniline hydroxylase and ethylmorphine *N*-demethylase associated with pregnancy in rats. J. Pharmacol. Exp. Ther. 168, 224–228.

He, X.J., Ejiri, N., Nakayama, H., Doi, K., 2005. Effects of pregnancy on CYPs protein expression in rat liver. Exp. Mol. Pathol. 78, 64–70.

Heil, S.H., Subramanian, M.G., 1998. Alcohol and the hormonal control of lactation. Alcohol Health Res. World 22, 178–184.

Lind, A.B., Wadelius, M., Darj, E., Finnstrom, N., Lundgren, S., Rane, A., 2003. Gene expression of cytochrome P450 1B1 and 2D6 in leukocytes in human pregnancy. Pharmacol. Toxicol. 92, 295–299.

Liu, P.T., Kentish, P.A., Symons, A.M., Parke, D.V., 1993. The effects of ether anaesthesia on oxidative stress in rats-dose response. Toxicology 80, 37–49.

Mannering, G.J., Deloria, L.B., 1986. The pharmacology and toxicology of the interferons: an overview. Annu. Rev. Pharmacol. Toxicol. 26, 455–515.

Neale, M.G., Parke, D.V., 1973. Effects of pregnancy on the metabolism of drugs in the rat and rabbit. Biochem. Pharmacol. 22, 1451–1461.

Pahan, K., Smith, B.T., Singh, A.K., Singh, I., 1997. Cytochrome P-450 2E1 in rat liver peroxisomes: downregulation by ischemia/reperfusion-induced oxidative stress. Free Radical Biol. Med. 23, 963–971.

Peristeris, P., Clark, B.D., Gatti, S., Faggioni, R., Mantovani, A., Mengozzi, M., Orencole, S.F., Sironi, M., Ghezzi, P., 1992. *N*-acetylcysteine and glutathione as inhibitors of tumor necrosis factor production. Cell. Immunol. 140, 390–399.

Smith, R.W., 1975. The effects of pregnancy and lactation on the activities in rat liver of some enzymes associated with glucose metabolism. Biochim. Biophys. Acta 411, 22–29.

Smith, J.L., Lear, S.R., Forte, T.M., Ko, W., Massimi, M., Erickson, S.K., 1998. Effect of pregnancy and lactation on lipoprotein and cholesterol metabolism in the rat. J. Lipid Res. 39, 2237–2249.

Spatling, L., Fallenstein, F., Huch, A., Huch, R., Rooth, G., 1992. The variability of cardiopulmonary adaptation to pregnancy at rest and during exercise. Br. J. Obstet. Gynaecol. 99, 1–40.

Symons, A.M., Turcan, R.G., Parke, D.V., 1982. Hepatic microsomal drug metabolism in the pregnant rat. Xenobiotica 12, 365–374.

Upreti, K., Chaki, S.P., Misro, M.M., 2002. Evaluation of peroxidative stress and enzymatic antioxidant activity during pregnancy and lactation in rats. Health Popul., Perspect. Issues 25, 177–185.

Williamson, D.H., 1986. Regulation of metabolism during lactation in the rat. Reprod. Nutr. Dev. 26, 597–603.

Available online at www.sciencedirect.com

SCIENCE DIRECT

Experimental and Molecular Pathology 78 (2005) 64–70

Experimental and Molecular Pathology

www.elsevier.com/locate/yexmp

Effects of pregnancy on CYPs protein expression in rat liver

Xi Jun He, Noriko Ejiri, Hiroyuki Nakayama, Kunio Doi*

Department of Veterinary Pathology, Graduate School of Agricultural and Life Sciences, The University of Tokyo, Japan

Received 16 August 2004
Available online 2 November 2004

Abstract

A body of evidence suggests that pregnancy may be responsible for the depression in the microsomal enzyme activity and the reduction in the total content of cytochrome P450 (CYP) in the rat liver. However, changes in expression of individual CYP isozyme remain poorly known. The current study was designed to examine the changes in CYPs protein expression in the liver of F344 rats in midpregnancy and late pregnancy by Western blot analysis and immunohistochemistry. Total nine antirat CYPs antibodies (CYP1A1, CYP2B1/CYP2B2, CYP2C6, CYP2C12, CYP2D1, CYP2D4, CYP2E1, CYP3A1, and CYP4A1) were used. In comparison with age-matched nonpregnant control rats, there were significant decreases in hepatic levels of CYP2B2, CYP2C6, and CYP4A1 in midpregnancy (day 13) and CYP2B2, CYP2C6, CYP4A1, CYP1A1, CYP2B1, and CYP2E1 in late pregnancy (day 19). The expression of CYP2C12, CYP2D1, and CYP 3A1 did not differ between nonpregnant and pregnant rats, and CYP2D4 was not detectable in microsomal proteins obtained from nonpregnant and pregnant rats at a protein loading of 20 μg total protein per lane. Immunohistochemistry showed that there were no differences in the distribution and degree of immunostainability for the abovementioned antibodies to nine CYPs between pregnant and nonpregnant rats.

Keywords: CYPs; F344 rat; Immunohistochemistry; Pregnancy; Western blot analysis

Introduction

Cytochrome P450 isozymes (CYPs) are the collective term for a large superfamily of heme-containing proteins that play an important role in the oxidative metabolism of numerous endogenous and foreign compounds (Nelson et al., 1996). Four of the CYP450 families, families CYP1 to CYP4, defined on the basis of their amino acid sequence similarities, are involved in drug metabolism and are preferentially expressed in the liver.

Expression of CYPs is known to be influenced by a variety of endogenous and foreign factors such as inflammation, age, gender, nutritional status, pregnancy, and chemical exposure. Pregnancy is a physiological state accompanied by a high metabolic demand. This appears to be involved in changes in activity of hepatic cytochrome CYPs monooxygenase. Previous studies have demonstrated that normal pregnancy is associated with a decrease in total CYP450 content and/or reduced activity of microsomal drug-metabolizing enzyme in the liver (Dean and Stock, 1975, 1989; Feuer and Liscio, 1969; Guarino et al., 1969; Neale and Parke, 1973). Change in total CYP450 content or drug metabolism, however, does not reflect changes in expression of individual CYPs, because CYPs metabolize xenobiotics and endogenous substances with differing affinities; that is, each individual CYP is characterized by diverse substrate specificity and significant differences in regulation. Genetic variability among individual family members further contributes to significant intersubject differences in metabolic capacity and pharmacological response (Rogers et al., 2002). To date, only few individual CYPs have been investigated during pregnancy. The findings obtained in hamsters have shown that in comparison to nonpregnant controls, pregnant hamsters showed

* Corresponding author. Department of Veterinary Pathology, Graduate School of Agricultural and Life Sciences, The University of Tokyo, Yayoi 1-1-1, Bunkyo-ku, Tokyo 113-8657, Japan. Fax: +81 3 5841 8185.
E-mail address: akunio@mail.ecc.u-tokyo.ac.jp (K. Doi).

0014-4800/$ - see front matter © 2004 Elsevier Inc. All rights reserved.
doi:10.1016/j.yexmp.2004.08.011

markedly decreased hepatic levels of both CYP2E and CYP2B mRNAs, which correlated with the results seen in immunoblot studies for these isozymes (Miller et al., 1992). Borlakoglu et al. (1993) investigated the alterations in rat hepatic drug metabolism during pregnancy and lactation. In their data, Western blot analysis of microsomal proteins obtained from pregnant rats shows that the expression of CYP1A1, CYP1A2, CYP2A1, CYP2B1, and CYP4A1 was not detectable in pregnant rats at a protein loading at 3 μg total protein per well. Casazza et al. (1994) demonstrated that CYP2E1 expression is suppressed in females particularly in late pregnancy in both acetone-treated and untreated rats by using immunoblot and Northern blot analyses. In human, there is an increase in activity of CYP2C6 enzyme during pregnancy, as assessed with dextromethorphan phenotyping test (Wadelius et al., 1997). This has been thought to be due to an induction of CYP2C6 enzyme. In the study by Czekaj et al. (2000), pregnancy was associated with decreased levels of CYP2B1/CYP2B2 protein in the liver in control and tobacco smoke-treated rats. Recently, Ejiri et al. (2001, 2003) investigated the changes in the expression and localization of CYPs protein in rat placenta at 9, 11, 13, 16, and 19 days of gestation by Western blot analysis and immunohistochemical staining. Only CYP3A1 was clearly detected during a long period of pregnancy.

According to the above-cited studies, changes in expression of most hepatic CYPs during rat pregnancy remain poorly known. In the present study, a total of nine CYPs throughout CYP1 to CYP4 subfamilies were designed to investigate the changes in expression in midpregnancy (day 13) and late pregnancy (day 19) by using Western blot analysis. The nine CYPs are thought to be concerned with drug-metabolizing system. CYP1A1 is involved in the oxidation of a wide spectrum of endogenous compounds and xenobiotics; CYP2B1 and CYP2B2 are involved in the activation of arenes, arylamines, and nitrosamine; CYP2C metabolizes the endogenous compound, arachidonic acid, and as such may play an important physiological role via the generation of bioactive eicosanoids; CYP2D has been shown to be one of determinants of polymorphic drug oxidations in human and rats, and it mainly catalyzes reaction of debrisoquine 4-hydroxylation; CYP2E1 is the major component of the microsomal ethal-oxidazing system (MEOS) and is responsible for the majority of acetone monooxygenase activity in rats; CYP3A catalyzes the 6β-hydroxylation of testosterone and metabolizes several drugs; CYP4A catalyzes the hydroxylation of the ω or ω-1 carbon of saturated and unsaturated fatty acids and prostaglandins.

In the present study, we also investigated the localization and distribution of these CYPs in the liver of pregnant and nonpregnant rats. The protocol of this study has been approved by the Animal Care and Use Committee of the Graduate School of Agricultural and Life Sciences, The University of Tokyo.

Materials and methods

Animals

Twelve pregnant and six age-matched nonpregnant female rats (11 weeks of age) were purchased from Saitama Experimental Animal Co. (Saitama, Japan) and used in this study. The day of a vaginal plug being recognized was designated as 0 day of gestation. The rats were individually housed in plastic cages in an animal room controlled at 23°C ± 2°C and at 55% ± 5% humidity condition with 14 h/10 h light/dark cycle, and fed pellets (MF, Oriental Yeast Co., Ltd., Tokyo, Japan) and water ad libitum. On days 13 and 19 of gestation, six dams were sacrificed. Livers were removed and used for Western blot analysis and immunohistochemical staining. Nonpregnant were used as controls.

Immunohistochemistry

Immunohistochemical staining for CYPs was carried out on the paraffin sections using a LSAB method with streptavidine (DAKO, Carpinteria, CA) (1:300). Monoclonal goat antirat CYP1A1, CYP2C6, CYP2E1, and CYP4A1 antibodies (Daiichi Pure Chemicals Co., Ltd., Tokyo, Japan) (1:200) and monoclonal rabbit antirat CYP2B1/2B2, CYP2C12, CYP2D1, CYP2D4, and CYP3A1 antibodies (Chemicon International Inc., Temecula, CA) (1:200) were used as the first antibody. Biotinylated antirabbit and antigoat antibodies (Kirkegaard and Perry Laboratories Inc., Gaithersburg, MD) (1:400) were used as the second antibody.

After having been deparaffinized, the sections were pretreated with trypsin solution (0.1% trypsin and 0.1% calcium chloride/Tris buffer) at 37°C for 30 min, then treated with 0.3% H_2O_2/methanol for 30 min to inactivate endogeneous peroxidase, and incubated in 8% skim milk/TBS at 37°C for 40 min to block nonspecific binding of the antibodies. The tissue sections were then incubated overnight at 4°C with the first antibodies diluted in 8% skim milk/TBS. Following washing in 3× TBS, the sections were incubated with the second antibodies for 30 min at room temperature and then in the streptavidine for 30 min. Finally, the sections were visualized by 0.05% 3,3′-diaminobenzidine (DAB) with 0.03% hydrogen peroxide in Tris HCl buffer, followed by counterstaining with methyl green.

Western blot analysis

Livers were homogenized in ice-cold 0.1 M phosphate buffer, pH 7.4, containing 150 mM KCl, 1 mM EDTA Na, and 1 mM DTT, and microsomes were prepared by differential centrifugation. Briefly, the liver homogenates were centrifuged at 9000 × *g* for 20 min at 4°C, and the resulting supernatant spun at 105,000 × *g* for 1 h at 4°C. After discarding the supernatant, the pellets were suspended in the same buffer and recentrifuged. The pellets were resuspended with 0.1 M PB, pH 7.4, containing 150 mM KCl, 20%

glycerol, 1 mM EDTA Na, and 1 mM DTT and stored at −80°C until used. Protein concentration of the samples was measured using bovine serum albumin (BSA) as the standard. Microsomal proteins (20 or 40 μl) were separated using SDS–PAGE in 10% polyacrylamide gels and electrophoretically transferred to polyvinylidene difluoride (PVDF) membrane (BIO-RAD, Richmond, CA), and the plate was blocked with 8% skim milk/TBS for 1 h at room temperature. The membrane was then incubated with the abovementioned antirat CYP1A1, CYP2B1/2B2, CYP2C6, CYP2C12, CYP2D1, CYP2D4, CYP2E1, CYP3A1, and CYP4A1 antibodies diluted in 8% skim milk/TBS (1:200) overnight at 4°C, followed by another 1-h incubation with horseradish peroxidase-conjugated secondary antibodies [donkey anti-rabbit IgG (Amersham Pharmacia Biotech Ltd., Arlington Heights, IL) and rabbit antigoat IgG (Cappel, Aurora, OH)]. The protein bands were visualized by ECL plus Western blotting detection system (Amersham Pharmacia Biotech Ltd.) followed by a brief exposure to Hyperfilm (Amersham Biosciences UK Ltd.). Quantity One v3.0 software (PDI, Inc., NY, USA) was used to quantitate the band intensities.

Statistical analysis

Results were presented as the mean ± standard deviation (SD). Student *t* test was employed to calculate the statistical significance between control and midpregnancy (day 13) or late pregnancy (day 19) groups.

Results

Change in body and liver weights

There were significant increases in the body and liver weights on day 19 of gestation (Table 1). On day 13 of gestation, there was no significant increase in the liver weight compared with nonpregnant controls, although there was a significant increase in maternal body weight (Table 1).

Findings of Western blot analysis

The results of Western blot analysis are shown in Figs. 1 and 2. The expression of CYP2C12, CYP2D1, and CYP 3A1 proteins did not differ between nonpregnant and pregnant (both days 13 and 19 of gestation) rats. CYP2D4 was not detectable in microsomal proteins obtained from nonpregnant and pregnant rats at a protein loading of 20 μg total protein per lane. Fig. 2 shows significant decreases in the CYP1A1, CYP2B1, and CYP2E1 contents in pregnant rats on day 19 of gestation (70.6%, 21.9%, and 61.0% of nonpregnant control values, respectively) and no significant change in pregnant rats on day 13 of gestation when compared with control. CYP2B2, CYP2C6, and CYP4A1 contents showed significant decreases on days 13 and 19 of gestation when compared with controls. Namely, on day 13 of gestation, CYP2B2, CYP2C6, and CYP4A1 proteins decreased to 29.2%, 67.4%, and 60.0% of control values, and on day 19 of gestation, they decreased to 25.8%, 69.8%, and 70.4% of control values, respectively.

Table 1
Body and liver weights

Gestation day	Body weight (g)	Liver weight (g)
Nonpregnant	144.35 ± 3.72	5.69 ± 0.39
Day 13 of gestation	161.83 ± 5.94*	6.06 ± 0.35
Day 19 of gestation	201.13 ± 8.66**	8.91 ± 0.19**

Data are represented as mean ± SD of 6 rats.
* $P < 0.01$; significantly different from controls.
** $P < 0.001$ significantly different from controls.

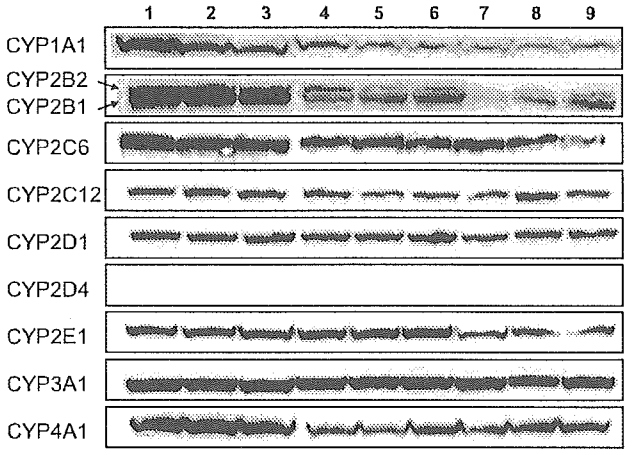

Fig. 1. Western blot analysis of liver microsomes from nonpregnant, midpregnant, and late pregnant rats. The amount of protein per lane was 20 μg (CYP2B1/2B2, CYP2C6 CYP2C12, CYP2D1, CYP2D4, CYP2E1, and CYP3A1) and 40 μg (CYP1A1 and CYP4A1). Lanes 1 to 3: Age-matched nonpregnant rats; lanes 4 to 6: midpregnant rats (day 13 of gestation); lanes 7 to 9: late pregnant rats (day 19 of gestation).

Immunohistochemical findings

Immunohistochemical analysis with antibodies to CYPs revealed that CYP1A1 was expressed in endothelial cells of both sinusoids and veins in the liver (Figs. 3a–c) There was a very slight expression of CYP4A1 in hepatocytes and endothelial cells in the liver. CYP2C6 (Figs. 3d–f), CYP2E1 (Figs. 3g–i), CYP 3A1 (Figs. 3j–l), and other CYPs were mainly expressed in centrilobular hepatocytes. CYP2D4 was not detectable in either pregnant or nonpregnant rat liver by immunohistochemical analysis. As shown in Fig. 3, there were no differences in the distribution and degree of immunostainability for antibodies against nine CYPs between pregnant and nonpregnant rat livers. Table 2 shows the distribution and degree of immunostainability for nine CYPs.

Discussion

In the present study, in comparison to age-matched nonpregnant control rats, pregnant rats showed significantly

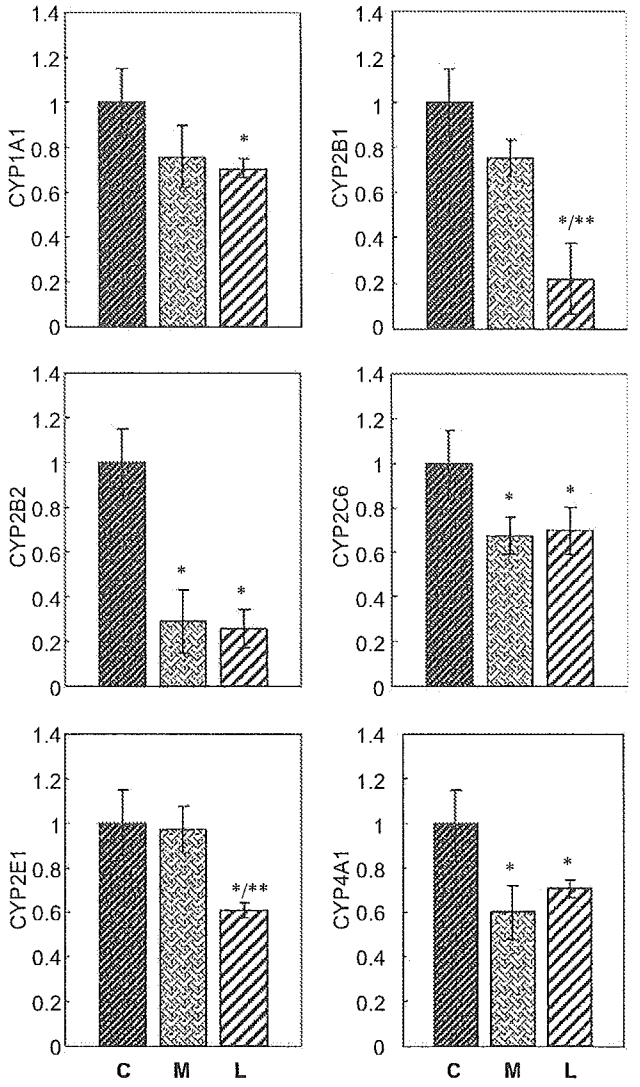

Fig. 2. Densitometry of Western blotting using monoclonal antibodies against rat hepatic CYP1A1, CYP2B1/2B2, CYP2C6, CYP2E1, and CYP4A1. Values are expressed as the ratio of pregnancy/nonpregnancy in arbitrary densitometric units of proteins amount and reported as the means ± SD of six rats. C indicates control nonpregnancy; M, midpregnancy; L, late pregnancy. *Significantly different from nonpregnant control at $P < 0.05$. **Significantly different from midpregnant rats at $P < 0.05$.

decreased hepatic levels of six out of nine CYPs proteins (CYP1A1, CYP2B1, CYP2B2, CYP2C6, CYP2E1, and CYP4A1) in midpregnancy (day 13) and/or late pregnancy (day 19).

Although, earlier reports have demonstrated that there was a decrease in rat hepatic total CYP450 content during pregnancy (Dean and Stock, 1975, 1989; Feuer and Kardish, 1975; Feuer and Liscio, 1969; Guarino et al., 1969), the mechanism of the effect of pregnancy on regulation of CYPs is still far from being fully clarified.

In the present study, pregnancy was linked to an increase in liver weight by up to 36.1% on day 19 of pregnancy. It has been hypothesized that a differential synthesis of hepatic proteins occurs during pregnancy, with little or no synthesis of the CYPs (Dean and Stock, 1975). It has also been thought that decrease in mixed-function oxidase activity during pregnancy is due to reduction in the hepatocellular capacity to metabolize drugs with an increase in liver size (Symons et al., 1982). However, in the present study, decreases in protein levels of CYPs (CYP2B2, CYP2C6, and CYP4A1) were not accompanied with an increase in liver weight, when detected in midpregnancy (day 13). Furthermore, Starkel et al. (2000) have demonstrated that early down-regulation of CYP3A and CYP2E1 in the regenerating rat liver is not related to the process of cellular proliferation. Therefore, liver enlargement might not be involved in the decrease in CYPs during rat pregnancy.

During pregnancy in rats, high plasma levels of both progesterone and its metabolites are produced. The depressed hepatic drug metabolism has been attributed to the pronounced hormonal changes that occur during pregnancy, in particular, to the higher plasma levels of both progesterone and its metabolites. Dean and Stock (1975) suggested that lower levels of hepatic microsomal enzyme activity might reflect a biological control mechanism to ensure the elevated levels of progesterone required to maintain the pregnant state. It has been known that the reduction in the activities of the microsomal drug-metabolizing enzymes in the rat is paralleled by a similar reduction in the total content of CYP450 (Dean and Stock, 1975; Feuer, 1979; Guarino et al., 1969; Neale and Parke, 1973). Thus, the increased production of progesterone and its metabolites can be implicated as a causative agent in pregnancy-induced regulation of CYPs; they seem to play a vital role in direct down-regulation of CYP450 expression and indirect reduction of the enzymatic activities.

Oxidative stress may be one of the factors which are responsible for the regulation of CYPs. In rats, lipid peroxidation remains low until midpregnancy and begins to rise after day 15 of pregnancy (Sugino et al., 1993). This role seems to be involved in our data; three out of nine CYPs decreased in midpregnancy (day 13), and up to six CYPs decreased in late pregnancy (day 19). Moreover, a measurable decrease in glutathione peroxidase in the liver and placenta, which play an important role in reducing the effects of oxidative stress in pregnancy, has been reported in pregnant rats (Mover-Lev and Ar, 1997). These observations indicate that there is an increase in oxidative stress during pregnancy. Oxidative stress has been suggested to result in the reduction of total CYP450 levels and drug metabolism activities in vivo (Gatti et al., 1993; Liu et al., 1993; Mannering and Deloria, 1986; Peristeris et al., 1992). Furthermore, Barker et al. (1994) have investigated the possibility that oxidative stress may influence inducer-dependent expression of CYP1A1 and CYP1A2, and demonstrated that hydrogen peroxide suppresses the accumulation of CYP1A1 and CYP1A2 mRNAs in isolated hepatocytes through a transcriptional mechanism. Pahan et al. (1997) demonstrated that there is a down-regulation of

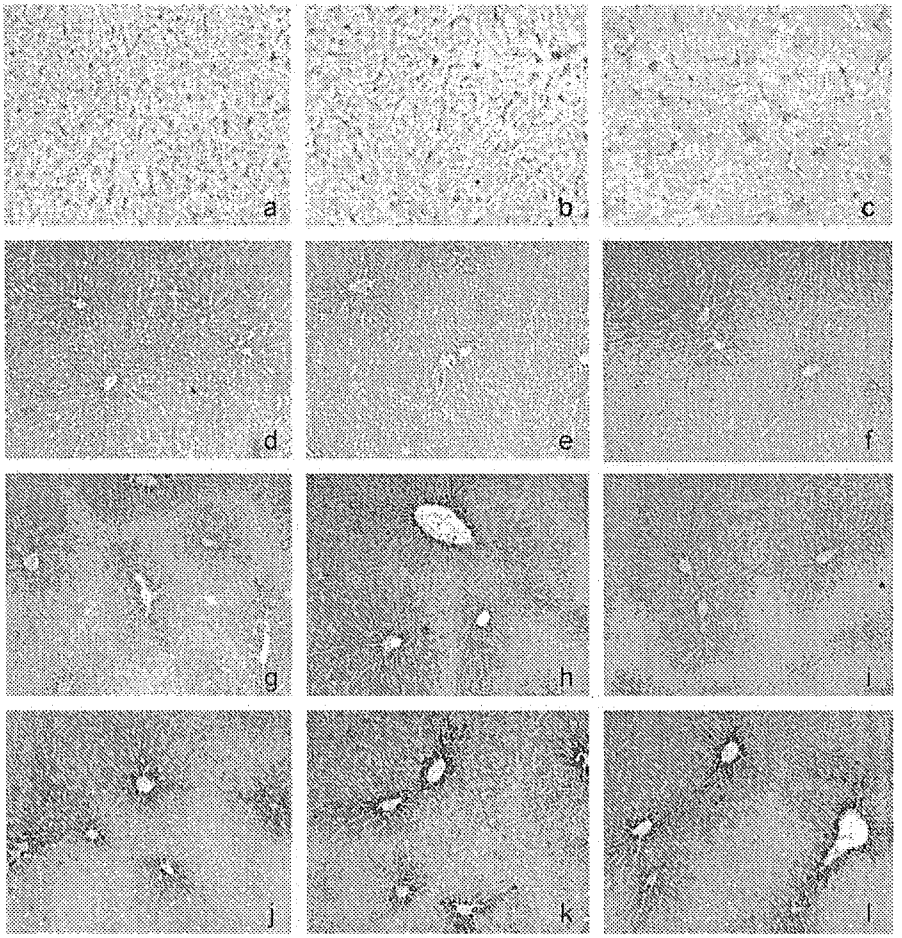

Fig. 3. Immunohistochemical distribution of CY1A1 (a–c), CYP2C6 (d–f), CYP2E1 (g–i), and CYP3A1 (j–l) proteins in the liver of nonpregnant rats (a, d, g, and j), midpregnant rats (b, e, h, and k), and late pregnant rats (c, f, i, and l). Immunostaining, magnification ×100.

CYP2E1 in rat liver peroxisomes by a mechanism of ischemia/reperfusion-induced oxidative stress. Decreases in CYP 1A1 and CYP2E1 protein levels in rat late pregnancy were also observed in the present study. Reduction of hepatic CYPs mRNAs expression during oxidative stress may be part of and adaptive response by the liver to minimize cell damage (Barke et al., 1994). To our knowledge, the relationship between CYPs expression and oxidative stress during pregnancy has not been investigated. It remains to be determined what extent changes in hepatic CYPs expression are regulated by increased oxidative stress during pregnancy.

Endogenous nitric oxide (NO), a potent vasodilator and a platelet antiaggregating factor, might also be involved in down-regulation of hepatic CYPs expression during rat pregnancy. Evidences provided by Conrad et al. (1993), McLaughlin and Conrad (1995), and Xu et al. (1996) show that the biosynthesis of NO increases during rat gestation as determined with plasma level and urinary excretion. Increased NO production has been suggested to play a role in the hemodynamic alterations of pregnancy (Xu et al., 1996). As one of the oxidative stresses, an increase in NO could also be thought to be an adaptive response during pregnancy by inhibiting CYP450 expression. Using human hepatocytes as an experimental model, Gonzalez (1990) demonstrated that exogenously added NO inhibited the CYP1A2 activity. In liver extracts, NO decreased the mRNA and protein expression of the phenobarbital-inducible CYP2B1 and CYP2B2 (Khatsenko et al., 1997), and it also decreased the constitutive expression of CYP3A2 (Minamiyama et al., 1997). In rat hepatocytes, high concentrations of bacterial lipopolysaccharide (LPS) evoked

Table 2
Distribution and degree of immunostainability for CYPs in the liver

CYPs	Cell type	
	Hepatocytes	Endothelial cells of sinusoids and veins
CYP1A1	–	++
CYP2B1/2	+	–
CYP2C6	++	–
CYP2C12	+++	–
CYP2D1	+++	–
CYP2D4	–	–
CYP2E1	++	–
CYP3A1	+++	–
CYP4A1	±	±

Note: –, negative; ±, very slight; +, slight; ++, moderate; +++, marked.

a rapid down-regulation of phenobarbital-induced CYP2B1 protein that was NO-dependent (Ferrari et al., 2001). Moreover, in a very recent study (Wang et al., 2003), it was demonstrated that a decrease in renal microsomal CYP4A1/CYP4A3 expression is dependent on NO in rat late pregnancy. These results, down-regulations of CYP2B1, CYP2B2, and CYP4A1 induced by NO, are partially consistent with our data. Therefore, these observations raise the possibility that NO may participate in down-regulation of hepatic CYPs during rat pregnancy. To date, it remains to be assessed that NO is involved in regulation of hepatic CYPs during rat pregnancy.

Pregnancy is a dynamic condition with major endocrine and physiological changes. At the present time, it is not clear how pregnancy regulates CYP450 expression. The abovementioned and other unknown mechanisms may be operating together to some extent, resulting in the decreased CYP450 expression. However, it should be pointed out that some CYPs were not affected during rat pregnancy, at least in the present study.

The localization and distribution of the CYP1A1, CYP2B1/2B2, CYP2C6, CYP2C12, CYP2D1, CYP2D4, CYP2E1, CYP3A1, and CYP4A1 proteins in the rat liver were also investigated by using immunohistochemistry with anti-CYPs antibodies. We observed that CYP1A1 is expressed in endothelial cells of both sinusoids and veins in the liver. The localization of CYP1A1 observed here confirms the findings of Annas and Brittebo (1998) who reported a colocalization of CYP1A1 immunoreactivity and covalent binding of 3H-Trp-P-1 in endothelial linings of capillaries and veins of heart, skeletal, muscle, and uterus in β-naphthoflavone (BNF)-treated rodents. Thus, endothelial cells appear to be the main cell type that expresses CYP1A1 in the rat liver. It has been suggested that CYP1A1 may be a factor in the regulation of vascular tone at these sites (Annas and Brittebo, 1998). CYP2B1/2B2, CYP2C6, CYP2C12, CYP2D1, CYP2E1, CYP3A1, and CYP4A1 were mainly expressed in centrilobular hepatocytes of hepatic acinus. This supports the general knowledge that most CYPs are expressed mainly in this region and some of them throughout the acinus in the rat liver. CYP4A1 was also detected in endothelial cells of both sinusoids and veins. We failed to show the CYP2D4 proteins in either pregnant or nonpregnant rat liver by using immunohistochemical staining.

In conclusion, the present study showed that pregnancy was associated with down-regulation of protein levels of CYP1A1, CYP2B1/2B2, CYP2C6, CYP2E1, and CYP4A1 in the rat liver but did not affect those of CYP2C12, CYP2D1, and CYP3A1. CYP1A1 and CYP4A1, especially the former, were expressed in endothelial cells of both sinusoids and veins. We are now conducting the study on the potential effects of oxidative stress and nitric oxide on the regulation of CYPs during pregnancy.

References

Annas, A., Brittebo, E.B., 1998. Localization of cytochrome P4501A1 and covalent binding of a mutagenic heterocyclic amine in blood vessel endothelia of rodents. Toxicology 129, 145–156.

Barker, C.W., Fagan, J.B., Pasco, D.S., 1994. Down-regulation of P4501A1 and P4501A2 mRNA expression in isolated hepatocytes by oxidative stress. J. Biol. Chem. 269, 3985–3990.

Borlakoglu, J.T., Scott, A., Henderson, C.J., Wolf, C.R., 1993. Alterations in rat hepatic drug metabolism during pregnancy and lactation. Biochem. Pharmacol. 46, 29–36.

Casazza, J.P., Sohn, D.H., Park, K.S., Song, B.J., 1994. Serum acetone and liver acetone monooxygenase activity in pregnant rats, fetuses, and neonates: reversible pretranslational reduction of cytochrome P450IIE1 (P450IIE1) during pregnancy. Arch. Biochem. Biophys. 309, 111–116.

Conrad, K.P., Joffe, G.M., Kruszyna, H., Kruszyna, R., Rochelle, L.G., Smith, R.P., Chavez, J.E., Mosher, M.D., 1993. Identification of increased nitric oxide biosynthesis during pregnancy in rats. FASEB J. 7, 566–571.

Czekaj, P., Wiaderkiewicz, A., Florek, E., Wiaderkiewicz, R., 2000. Expression of cytochrome CYP2B1/2 in nonpregnant, pregnant and fetal rats exposed to tobacco smoke. Acta Biochim. Pol. 47, 1115–1127.

Dean, M.E., Stock, B.H., 1975. Hepatic microsomal metabolism of drugs during pregnancy in the rat. Drug Metab. Dispos. 3, 325–331.

Dean, M.E., Stock, B.H., 1989. The influence of phenobarbital administration on hepatic monooxygenase activity at various stages of gestation in the rat. Drug Metab. Dispos. 17, 579–581.

Ejiri, N., Katayama, K.I., Nakayama, H., Doi, K., 2001. Expression of cytochrome P450 (CYP) isozymes in rat placenta through pregnancy. Exp. Toxicol. Pathol. 53, 387–391.

Ejiri, N., Katayama, K., Doi, K., 2003. Induction of CYP3A1 by dexamethasone and pregnenolone-16 alpha-carbonitrile in pregnant rat and fetal livers and placenta. Exp. Toxicol. Pathol. 54, 273–279.

Ferrari, L., Peng, N., Halpert, J.R., Morgan, E.T., 2001. Role of nitric oxide in down-regulation of CYP2B1 protein, but not RNA, in primary cultures of rat hepatocytes. Mol. Pharmacol. 60, 209–216.

Feuer, G., 1979. Action of pregnancy and various progesterones on hepatic microsomal activities. Drug Metab. Rev. 9, 147–169.

Feuer, G., Kardish, R., 1975. Hormonal regulation of drug metabolism during pregnancy. Int. J. Clin. Pharmacol. Biopharm. 11, 366–374.

Feuer, G., Liscio, A., 1969. Origin of delayed development of drug metabolism in the newborn rat. Nature 223, 68–70.

Gatti, S., Faggioni, R., Echtenacher, B., Ghezzi, P., 1993. Role of tumour necrosis factor and reactive oxygen intermediates in lipopolysaccharide-induced pulmonary oedema and lethality. Clin. Exp. Immunol. 91, 456–461.

Gonzalez, F.J., 1990. Molecular genetics of the P-450 super family. Pharmacol. Ther. 45, 1–38.

Guarino, A.M., Gram, T.E., Schroeder, D.H., Call, J.B., Gillette, J.R., 1969. Alterations in kinetic constants for hepatic microsomal aniline hydroxylase and ethylmorphine *N*-demethylase associated with pregnancy in rats. J. Pharmacol. Exp. Ther. 168, 224–228.

Khatsenko, O.G., Boobis, A.R., Gross, S.S., 1997. Evidence for nitric oxide participation in down-regulation of CYP2B1/2 gene expression at the pretranslational level. Toxicol. Lett. 90, 207–216.

Liu, P.T., Kentish, P.A., Symons, A.M., Parke, D.V., 1993. The effects of ether anaesthesia on oxidative stress in rats—dose response. Toxicology 80, 37–49.

Mannering, G.J., Deloria, L.B., 1986. The pharmacology and toxicology of the interferons: an overview. Ann. Rev. Pharmacol. Toxicol. 26, 455–515.

McLaughlin, M.K., Conrad, K.P., 1995. Nitric oxide biosynthesis during pregnancy: implications for circulatory changes. Clin. Exp. Pharmacol. Physiol. 22, 164–171.

Miller, M.S., Warner, S.P., Jorquera, R., Castonguay, A., Schuller, H.M., 1992. Expression of the cytochrome P4502E and 2B gene families in the lungs and livers of nonpregnant, pregnant, and fetal hamsters. Biochem. Pharmacol. 44, 797–803.

Minamiyama, Y., Takemura, S., Imaoka, S., Funae, Y., Tanimoto, Y., Inoue, M., 1997. Irreversible inhibition of cytochrome P450 by nitric oxide. J. Pharmacol. Exp. Ther. 283, 1479–1485.

Mover-Lev, H., Ar, A., 1997. Changes in enzymatic antioxidant activity in pregnant rats exposed to hyperoxia or hypoxia. Comp. Biochem. Physiol. 118, 353–359.

Neale, M.G., Parke, D.V., 1973. Effects of pregnancy on the metabolism of drugs in the rat and rabbit. Biochem. Pharmacol. 22, 1451–1461.

Nelson, D.R., Koymans, L., Kamataki, T., Stegeman, J.J., Feyereisen, R., Waxman, D.J., Waterman, M.R., Gotoh, O., Coon, M.J., Estabrook, R.W., Gunsalus, I.C., Nebert, D.W., 1996. P450 superfamily: update on new sequences, gene mapping, accession numbers and nomenclature. Pharmacogenetics 6, 1–42.

Pahan, K., Smith, B.T., Singh, A.K., Singh, I., 1997. Cytochrome P-450 2E1 in rat liver peroxisomes: downregulation by ischemia/reperfusion-induced oxidative stress. Free Radical Biol. Med. 23, 963–971.

Peristeris, P., Clark, B.D., Gatti, S., Faggioni, R., Mantovani, A., Mengozzi, M., Orencole, S.F., Sironi, M., Ghezzi, P., 1992. *N*-acetylcysteine and glutathione as inhibitors of tumor necrosis factor production. Cell. Immunol. 140, 390–399.

Rogers, J.F., Nafziger, A.N., Bertino Jr., J.S., 2002. Pharmacogenetics affects dosing, efficacy, and toxicity of cytochrome P450-metabolized drugs. Am. J. Med. 113, 746–750.

Starkel, P., Laurent, S., Petit, M., Van Den Berge, V., Lambotte, L., Horsmans, Y., 2000. Early down-regulation of cytochrome P450 3A and 2E1 in the regenerating rat liver is not related to the loss of liver mass or the process of cellular proliferation. Liver 20, 405–410.

Sugino, N., Nakamura, Y., Takeda, O., Ishimatsu, M., Kato, H., 1993. Changes in activities of superoxide dismutase and lipid peroxide in corpus luteum during pregnancy in rats. J. Reprod. Fertil. 97, 347–351.

Symons, A.M., Turcan, R.G., Parke, D.V., 1982. Hepatic microsomal drug metabolism in the pregnant rat. Xenobiotica 12, 365–374.

Wadelius, M., Darj, E., Frenne, G., Rane, A., 1997. Induction of CYP2D6 in pregnancy. Clin. Pharmacol. Ther. 62, 400–407.

Wang, M.H., Wang, J., Chang, H.H., Zand, B.A., Jiang, M., Nasjletti, A., Laniado-Schwartzman, M., 2003. Regulation of renal CYP4A expression and 20-HETE synthesis by nitric oxide in pregnant rats. Am. J. Physiol.: Renal. Physiol. 285, F295–F302.

Xu, D.L., Martin, P.Y., St. John, J., Tsai, P., Summer, S.N., Ohara, M., Kim, J.K., Schrier, R.W., 1996. Upregulation of endothelial and neuronal constitutive nitric oxide synthase in pregnant rats. Am. J. Physiol. 271, R1739–R1745.

Available online at www.sciencedirect.com
SCIENCE DIRECT®
Neurotoxicology and Teratology 28 (2006) 125 – 134
NEUROTOXICOLOGY AND TERATOLOGY
www.elsevier.com/locate/neutera

Molecular mechanisms of hydroxyurea(HU)-induced apoptosis in the mouse fetal brain

G.H. Woo [a], E.J. Bak [b], H. Nakayama [a], K. Doi [a,*]

[a] *Department of Veterinary Pathology, Graduate School of Agricultural and Life Sciences, The University of Tokyo, 1-1-1 Yayoi, Bunkyo-ku, Tokyo 113-8657, Japan*
[b] *Department of Biomedical Science, Graduate School of Agricultural and Life Sciences, The University of Tokyo, Japan*

Received 8 March 2005; received in revised form 26 July 2005; accepted 4 August 2005
Available online 13 December 2005

Abstract

Hydroxyurea (HU), a potent mammalian teratogen, affects proliferating embryonic cells and inhibits DNA synthesis. The teratogenic potential of HU has been well known in experimental animals for several decades. In this study, we investigated molecular mechanisms of HU-induced apoptosis in the telencephalon of the fetal brain by exposing pregnant mice to HU on day 13 of gestation. The number of TUNEL-positive cells began to increase at 3 h, peaked at 12 h, and rapidly decreased at 24 h. Although changes of *p53* mRNA expression were not observed by RT-PCR, a p53-positive reaction was detected immunohistochemically in the nuclei of neuroepithelial cells from 1 h to 6 h, and p53-protein expression was simultaneously identified by Western blot analysis. The expression of p53-target genes was detected at both the mRNA and protein. The mRNA levels of apotosis-related genes (*fas*, *fasL*, and *bax*) and cell cycle-related genes (*mdm2* and *p21*) were significantly elevated, and the degree to and sequence in which these target genes expressed was similar to those for fas, fasL, mdm2 and p21. Flow-cytometric and Western blot analyses of cell cycle-related proteins suggested that neuroepithelial cells are arrested at the S checkpoint from 3 to 6 h and at the G2/M checkpoint at 12 h, respectively. HU-induced apoptosis is considered to be mediated by p53 in the fetal brain.

Keywords: Apoptosis; p53; Cell arrest; Hydroxyurea; Fetus; Mouse

1. Introduction

Apoptosis is involved in developmental phenomena and processes such as sculpting structures, deleting unneeded structures and eliminating abnormal, misplaced, non-functional or harmful cells. It occurs as early as the blastocyst stage of development, during the formation of extraembryonic tissues, and continues throughout organogenesis [15]. It is important to emphasize that an association between excessive apoptosis and maldevelopment was observed in embryos exposed to detrimental stimuli at both pre-and post-implantation stages of development. We observed the largest cluster of TUNEL-positive nuclei in the neuroepithelium of the central nervous system (CNS) and mesenchymal cells in the lung, craniofacial tissues and limb buds of fetuses obtained from pregnant mice administrated with hydroxyurea (HU) on day 13 of gestation [39].

p53 can be activated by DNA damage, hypoxia, or aberrant oncogene expression to promote progression through cell-cycle checkpoints, DNA repair, cellular senescence, and apoptosis. Numerous studies have indicated that p53 plays a key role in apoptotic cell death following certain types of toxic stress [18,22,36,37]. Active p53 functions as a transcriptional transactivator and transrepressor, and contributes to a variety of protein–protein interactions [26]. Cell cycle arrest mediated by p53 is clearly correlated with the function of p53 as a transcriptional transactivator of genes, such as those for p21 and a cyclin-dependent kinase inhibitor.

HU is a well-known experimental teratogen and ultimately induces apoptotic cell death by a specific inhibition of DNA synthesis without any effect on RNA or protein synthesis [41]. In this study, the sequential changes in the expression of a p53-transcriptional transactivator and transrepressor were investigated in order to elucidate the molecular regulatory mechan-

* Corresponding author. Tel./fax: +81 3 5841 8185.
E-mail address: akunio@mail.ecc.u-tokyo.ac.jp (K. Doi).

0892-0362/$ - see front matter © 2005 Elsevier Inc. All rights reserved.
doi:10.1016/j.ntt.2005.08.002

isms of HU-induced apoptosis in the fetal brain. The protocol of the present study was approved by the Animal Use and Care Committee of the Graduate School of Agricultural and Life Sciences, the University of Tokyo.

2. Methods

2.1. Animals

Eighty-four 8-week-old pregnant mice of the Crj:CD-1(ICR) strain were obtained from Charles River Japan Co., Yokohama, Japan. They were kept in an animal room under controlled conditions (temperature, 23±2 °C; relative humidity, 55±5%) using an isolator caging system (Niki Shoji, Co., Tokyo) and were fed commercial pellets (MF, Oriental Yeast Co., Tokyo) and water ad libitum.

2.2. Chemicals

Hydroxyurea (HU) (Sigma, St. Louis, MO) was dissolved in distilled water immediately before use, and adjusted to a concentration of 60 mg/ml. BrdU (Sigma, St. Louis, MO) was also dissolved in physiologic saline immediately before use, at a concentration of 4 mg/ml.

2.3. Treatments

Forty-eight pregnant mice were injected with 400 mg/kg b.w. of HU intraperitoneally (i.p.) at day 13 of gestation (date vaginal plug found=day 0), and 8 dams each were sacrificed by heart puncture under ether anesthesia at 1, 3, 6, 12, 24, and 48 h after the treatment (h). Another thirty-six pregnant mice were injected i.p. with distilled water (DW), and six dams each were sacrificed in the same way. BrdU at 20 mg/kg b.w. was injected i.p. into 8 dams at each time point as well as 3 dams as controls for histopathology, immunohistochemistry and RT-PCR at 1 h before necropsy, and simultaneously with HU into 6 dams at each time point along with 3 dams as controls for Western blotting and flow cytometry.

2.4. Histopathology

Fetuses were collected by Caesarian section and fixed in 10% neutral-buffered formalin. Paraffin sections (4 μm) were stained with hematoxylin and eosin (HE). Some of the paraffin sections were subjected to immunohistochemical staining for TUNEL, p53, cleaved caspase 3 and BrdU as mentioned below.

2.5. In situ detection of fragmented DNA

DNA fragmentation was examined in the paraffin sections using the modified TUNEL method first proposed by Gravieli et al. [11], with a commercial kit (ApopTag In situ Apoptosis Detection Kit; Oncor, Gaithersburg, MD). In brief, the procedure was as follows: multiple fragmented 3′-OH ends were labeled with digoxigenin-dUTP in the presence of terminal deoxynucleotidyl transferase (TdT). Peroxidase-conjugated anti-digoxigenin antibody was then reacted with the sections. Apoptotic nuclei were visualized using peroxidase-diaminobenzidine (DAB) reaction. The sections were then counterstained with methylgreen. TUNEL-positive cells in the telencephalon were counted under a light microscope (×400). A 10×10 squared grid eyepiece was used to designate the sample field (0.0625 mm^2). The total number of positive cells was recorded from 3 randomly chosen microscope fields on each telencephalon. The average number of positive cells per field was divided by a conversion factor of 0.0625 mm^2, and the number of TUNEL positive cells was calculated. The number of TUNEL-positive cells/mm^2 was expressed as the mean±standard deviation (SD) for 5 dams (5 fetuses/dam) at each point of examination.

2.6. Immunohistochemistry

Paraffin sections of fetuses were deparaffinized and hydrated in a series of descending ethanol concentrations finishing with distilled water. For the detection of p53, sections were immersed in 10 mM citrate buffer, pH 6.0, and autoclaved for 10 min at 120 °C. After washing in tris-buffered saline (TBS), endogenous peroxidase activity was quenched for 30 min in 0.3 % H_2O_2 in methanol and the sections were washed 3 times with TBS. The sections were incubated in 8% skim milk for 40 min at 37 °C to reduce non-specific staining, and then immediately with rabbit antibody against p53 (1:300; Santa Cruz) in TBS overnight at 4 °C. After washing in TBS, sections were incubated with Envision kit (Dako, Carpinteria, CA) for 30 min at room temperature (RT), and then washed in TBS. The sections were visualized using the peroxidase-DAB reaction and then counterstained with methyl green. For the detection of cleaved caspase 3, sections were immersed in 10 mM citrate buffer, pH 6.0, and autoclaved for 10 min at 120 °C. After washing in TBS, endogenous peroxidase activity was quenched for 30 min in 0.3% H_2O_2 in methanol and the sections washed 3 times with TBS. The sections were incubated in 8% skim milk for 40 min at 37 °C to reduce non-specific staining, and then immediately in rabbit antibody against cleaved caspase 3 (1:200; Cell signaling) in TBS overnight at 4 °C. After washing in TBS, sections were incubated with biotinylated antibody against rabbit IgG (1:400; Kirkegaard and Perry, Gaitherburg, MD) according to the manufacturer's instructions, then washed in TBS and incubated with streptavidine (1:300; Dako). The sections were visualized using the peroxidase-DAB reaction and then counterstained with methyl green and coverslipped. For the detection of BrdU, sections were treated with 0.1% trypsin and 0.1% calcium chloride in Tris buffer at 37 °C and 1 N HCl at RT for 30 min each. After washing in TBS, endogenous peroxidase activity was quenched for 30 min in 0.3% H_2O_2 in methanol, and the sections were washed 3 times with TBS. The sections were incubated in 8% skim milk for 40 min at 37 °C to reduce non-specific staining, and then immediately with mouse antibody against BrdU (1:100; Dako) in TBS overnight at 4 °C. After being washed in TBS, the sections were incubated with

biotinylated antibody against mouse IgG (1:400; Kirkegaard and Perry, Gaitherburg, MD) according to the manufacturer's instructions, washed in TBS, and then incubated with streptavidine (1:300; Dako).

Positive cells in the telencephalon were counted under a light microscope (×400). The number of positive cells/mm^2 was expressed as the mean±standard deviation (SD) for 5 dams (5 fetuses/dam) at each point of examination, and a statistical analysis was done with Student's *t*-test comparing the control and HU-treated groups.

2.7. Western blotting

Embryo telencephalons were microdissected from five fetuses each of 3 dams and were frozen on dry ice. Whole embryo telencephalons were pooled and lysed in a buffer containing 50 mM Tris–HCl (pH 8.0), 150 mM NaCl, 0.02% sodium azide, 0.1% SDS, 1% NP-40, 0.5% sodium deoxycholate, 1 mM PMSF, 2 μg/ml aprotinin, 2 μg/ml leupeptins, 100 mM Na_3VO_4, and 10 mM NaF. Protein concentrations in the lysates were determined using the Bio-Rad protein assay. Samples containing equal amounts of protein were separated on 10% SDS polyacrylamide gels and blotted onto nitrocellulose membranes. Membranes were blocked in TBS containing 0.1% Tween-20 and 2.5% skim milk before the addition of antibodies. The primary antibodies used were anti-p53 (1:500; Santa Cruz), anti-p21 (1:500; PharMingen), anti-fas (1:500; Santa Cruz), anti-fasL (1:500; Santa Cruz), anti-bax (1:500; Santa Cruz), anti-cyclin B1 (1:500; Santa Cruz), anti-cyclin D1 (1:500; Dako), anti-cdk4 (1:500; Santa Cruz), anti-chk2 (1:500; Santa Cruz), anti-cyclin G1 (1:500; Santa Cruz), anti-mdm2 (1:100; Santa Cruz), anti-phospho-p53-ser 15 (1:500; Cell signaling), anti-phospho-p53-ser 20 (1:500; Cell signaling), anti-phospho-cdc2 (1:500; Cell signaling), anti-phospho-Rb (1:500; Cell signaling), and anti-β-actin (1:10000; Sigma). Horseradish peroxidase-conjugated secondary antibodies (anti-mouse or anti-rabbit; Amersham) were used at a dilution of 1:10000. Enhanced chemiluminescence (ECL+; Amersham) was used for signal detection before exposing blots to film.

2.8. RNA extraction and RT-PCR analysis

Telencepholons of five fetal heads from each dam were pooled and total cellular RNA was extracted from each homogenized sample using the Isogen kit (Nippon Gene, Toyama, Japan). The reverse transcription (RT) reaction for synthesizing the first strand cDNA was carried out using an oligo(dT)$_{12-18}$ primer and SUPERSCRIPT™ II Rnase H$^-$ Reverse Transcriptase (Gibco, Gaithersburg, MD). PCR was performed using oligonucleotide primers sets corresponding to the cDNA sequences of p53, its transcriptional target genes (*p21, apaf-1, bax, fas, cyclin G*, and *mdm2*), *fas L*, and *glyceraldehyde-3-phosphate dehydrogenase* (*GAPDH*) (Table 1). To determine optimized PCR cycles to achieve template amplification within exponential phase in the mouse telencephalon, validation PCR experiments by setting graded cycles from 26 to 42 were preliminary performed. PCR amplifications were performed in 50 μl of reaction mixture containing 5 μl 10× PCR buffer (100 mM Tris–HCl buffer, 500 mM KCl, and 15 mM $MgCl_2$;Takara, Shiga, Japan), 5 μl dNTP (Takara), 1.25 U of Taq™, 50 pM each of sense and antisense primer, and 1 μl of cDNA. After an initial denaturation at 94 °C for 7 min, amplification was performed in a Takara PCR Thermal cycler SP (Takara) for each cycles (Table 1) under the following conditions: 1 min of denaturation at 94 °C, 2 min (fas and fasL) or 1 min (the others) of annealing at 64 °C (fas and fasL) or 58.5 °C (the others), and 3 min (fas and fasL) or 1 min (the others) of extension at 72 °C. Amplification of GAPDH mRNA was used to control the concentration of template loaded. The PCR products were electrophoretically separated in 2% agarose S (Nippon Gene) in TBE buffer (89 mM Tris–aminomethane, 89 mM Boric acid, and 10 mM EDTA). The gels were stained with ethidium bromide (Gibco). Fluorescent bands were visualized using a UV-CCD video system (EpiLight$_{UVFA1100}$; AISIN COSMOS, Tokyo, Japan) and were analyzed using an image-analysis software, Quantity One (pdi, NY). The intensity of the band relative to the GAPDH band was represented as the mean±standard error (SE). The significance of differences between the control group and HU-treated group was evaluated with Student's *t*-test or Welch's *t*-test. For all genes, PCR cycle conditions were predetermined to give amplification within the linear range using control samples.

2.9. Flow cytomery

For the assessment of sub-G1 DNA content, the cells were prepared in two fetal telencephalons, washed in PBS, and

Table 1
Oligonucleotide primers for each molecule and cycle numbers

Gene	Sense(5′–3)	Antisense(5′–3)	Cycle numbers
p53	GCCAGGAGACATTTTCAGGC	AACTGCACAGGGCACGTCTT	31
p21	AATCCTGGTGATGTCCGACC	GACCAATCTGCGCTTGGAGT	32
fas	GCTCAGAAGGGAAGGAGTAC	ACTGGAGGTTCTAGATTCAGG	35
fasL	TAGACAGCAGTGCCACCACTTCAT	AACTCACGGAGTTCTGCCAGTT	39
bax	TTCATCCAGGATCGAGCAGG	TGAGGACTCCAGCCACAAAGAT	30
Apaf-1	GACTGTTGGACCGTGGCATT	CCAAGCCCTCGGAATCTTTC	37
mdm2	CATCAGGATCTTGACGATGGC	GGAGAAGCTAGATTCCACACTCT	31
Cyclin G	CTTTGGCTTTGACACGGAGAC	GGAATCGTTGGGAGGTGAGTT	33
GAPDH	TGATGGGTGTGAACCACGAG	TTGAAGTCGCAGGAGACAACC	29

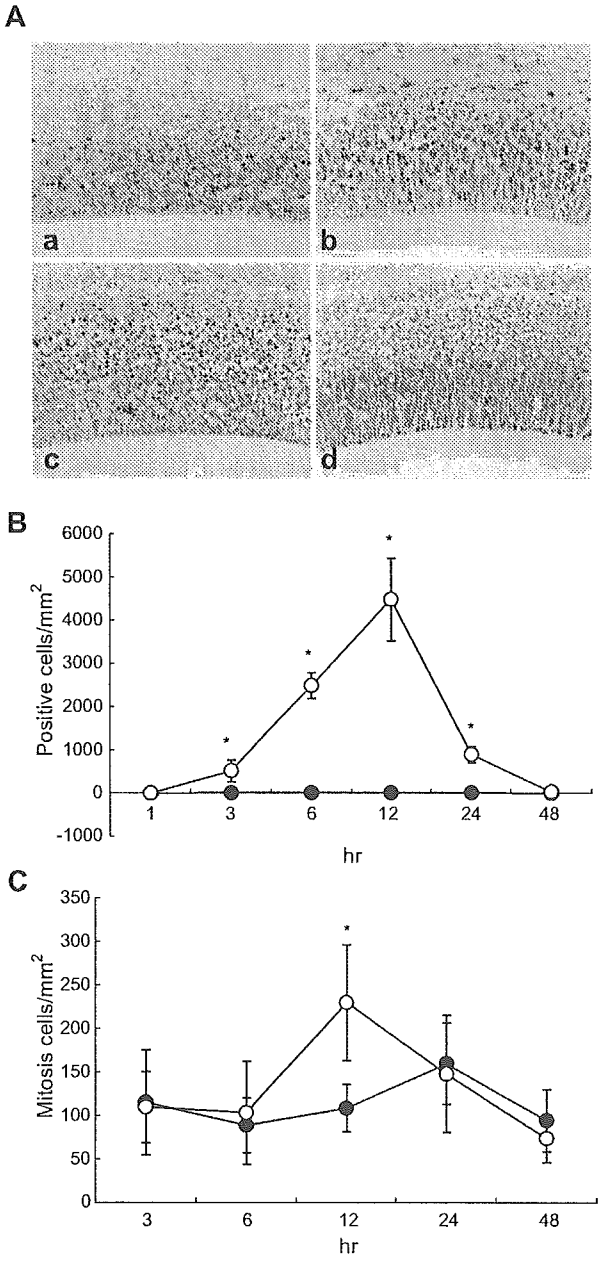

Fig. 1. Immunohistochemical staining for TUNEL. (A) TUNEL-positive cells in the telencephalon of fetuses of the HU-treated group at 3 (a), 6 (b) and 12 h (c), and of a fetus of the control group at 12 h (d). TUNEL-positive cells were mainly observed in the middle layer of the ventricular zone at 3 h, and in the middle to dorsal layers at 12 h. ×300. (B) Changes in the number of TUNEL-positive cells in the fetal telencephalon in the HU-treated (○) and control groups (●). Each value represents the mean±SD for 5 dams. The number of TUNEL-positive cells began to increase at 3 h, peaked at 12 h, and decreased at 24 h. *$p<0.01$, significantly different from the control group using Student's t-test. (C) Changes in the number of mitotic cells in the fetal telencephalon in the HU-treated (○) and control groups (●). Significant increase in the number of mitotic cells was observed in the inner layer of the ventricular zone at 12 h. See note in (B).

resuspended in 1 ml of PBS at a density of 1×10^6 cells/ml. An amount of 2.7 ml of ice-cold ethanol was added to a final ethanol concentration of 70%. After centrifugation, the cells were resuspended in 1 ml of PBS and incubated with 10 μl of RNAse for 40 min at 37 °C. An amount of 10 μl of propidium-iodide (5 mg/ml) was added. FSC and SSC analysis was performed to assess changes in cell morphology, and FL-2H analysis to detect changes in DNA content and DNA fragmentation using a FACScalibur machine (Becton-Dickson, Franklin Lakes, NJ).

For the assessment of cell cycle kinetics, the cells were fixed, washed with PBS and resuspended in 0.5% Triton X-100 in 2 N HCl for 30 min at RT. Following neutralization with 0.1 M $Na_2B_4O_7$, they were pelleted and washed with PBS. Cells were then stained with FITC-conjugated mouse anti-BrdU antibody (BD PharMingen) for 30 min in the dark at RT. They were then washed with 0.5% Tween 20 and 1% BSA in PBS, incubated with 2 μl of propidium iodide for 30 min on ice, and analyzed using the FACScalibur machine.

3. Results

3.1. Immunohistochemical findings

Results of TUNEL labeling of the fetal telencephalon are shown in Fig. 1A and B. The number of positive cells began to increase at 3 h (Fig. 1Aa), gradually increased at 6 h (Fig. 1Ab), and peaked at 12 h (Fig. 1Ac). The number of mitotic cells in the inner layer of the ventricular zone significantly increased at 12 h as compared with the control (Fig. 1C), and the change in the number of cleaved caspase 3-positive cells corresponded well to that in TUNEL-positive cells (Fig. 2). Changes in the number of p53-positive cells are shown in Fig. 3. A lot of positive cells were detected from 1 h (Fig. 3Aa) and there was no significant difference between the number at 1 h and 3 h (Fig. 3Ab). Positive cells rapidly decreased at 6 h (Fig. 3B), and returned to the control level at 12 h (Fig. 3Ac and B).

The results of BrdU labeling of the fetal telencephalon are shown in Fig. 4. The number of BrdU-positive cells significantly decreased at 3 and 12 h.

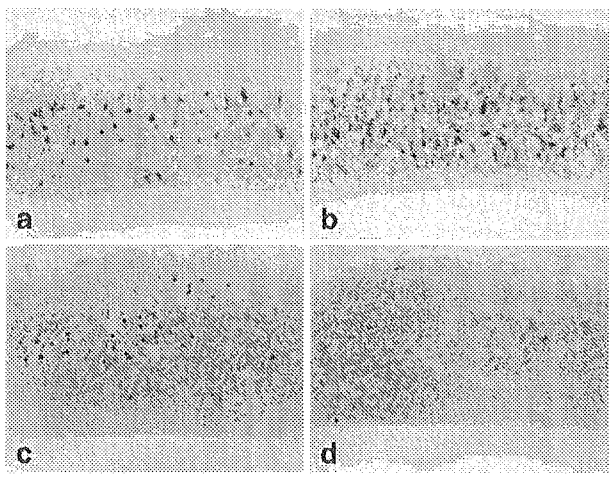

Fig. 2. Immunohistochemical staining for cleaved caspase 3 in the telencephalon of fetuses of the HU-treated group at 3 (a), 12 (b) and 24 h (c), and of a fetus of the control group at 12 h (d). The number of cleaved caspase 3-positive cells began to increase at 3 h, peaked at 12 h, and decreased at 24 h. ×300.

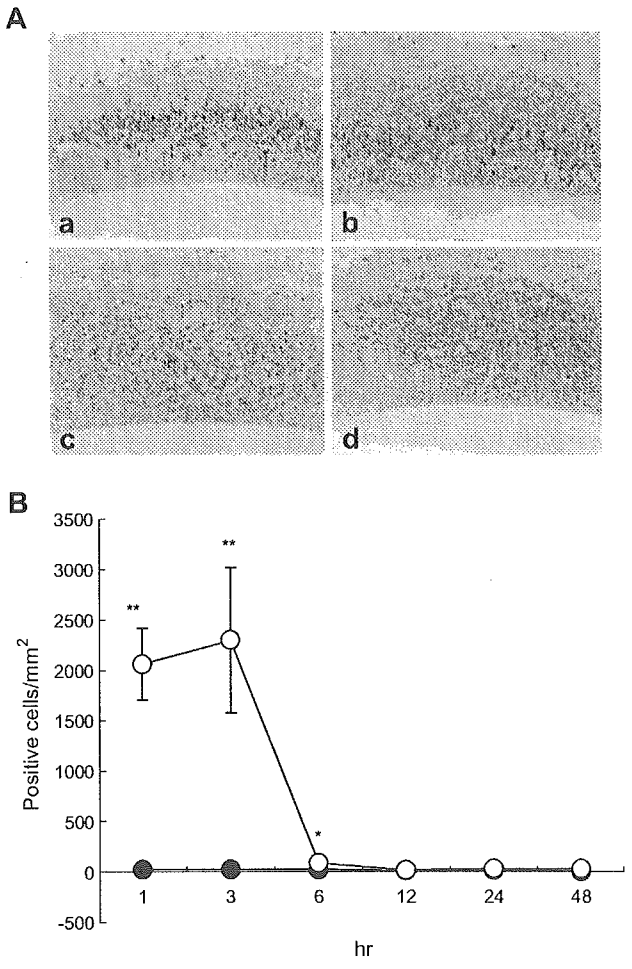

Fig. 3. Immunohistochemical staining for p53. (A) p53-positive cells in the telencephalon of fetuses of the HU-treated group at 1 (a), 3 (b) and 12 h (c), and of a fetus of the control group at 12 h (d). p53-positive cells were mainly observed in the middle layer of the ventricular zone at 1 and 3 h. ×300. (B) Changes in the number of p53-positive cells in the fetal telencephalon in the HU-treated (○) and control groups (●). Lots of p53-positive cells were observed at 1 and 3 h. p53-positive cells rapidly decreased at 6 h and returned to the control level at 12 h. Each value represents the mean±SD for 5 dams. *$p<0.05$, **$p<0.01$; significantly different from the control using Student's *t*-test.

3.2. Western blotting analysis

The results of the Western blot analysis on the expression levels of apoptosis and cell cycle arrest-related proteins (p53 and phosphorylated-p53 (Ser 15 and Ser 20), p21, bax, fas, fasL, cyclin G1, mdm2, phosphorylated-Rb, phosphorylated-cdc, cdk4, chk2, cyclin D1, and cyclin B1) in the fetal telencephalon are shown in Fig. 5.

The expression of p53 gradually increased at 12 h and decreased thereafter. Furthermore, phosphorylation of p53 at Ser 15 and Ser 20, associated with reduced interaction of p53 with mdm2, was strongly detected at 3 h. The expression of p53-transcriptional target proteins (fas, bax, cyclin G1, and p21) was seen. And fasL protein was expressed from 1 to 12 h.

The expression of mdm2 protein, a key mediator of p53 protein stability, gradually decreased to 6 h, but began to increase at 12 h.

Also, we evaluated protein expression associated with the G1/S checkpoint (cyclin D1, cdk4 and phospho-Rb) and G2/M checkpoint (cyclin B1, chk2 and phospho-cdc2). The expression of cylin D1 and cdk4 proteins decreased at 6 h. The expression of cyclin B1 protein began to decrease at 3 hr and was weakly detected at 12 h.

3.3. Findings of RT-PCR

RT-PCR analysis of the mRNA for apoptosis-associated genes in homogenates of pooled samples of the fetal telencephalon are shown in Fig. 6. The expression of *fas* mRNA significantly increased at 3–12 h as compared with that in the control group (Fig. 6). The level of *fasL* mRNA was significantly elevated from 6 h to 12 h. A significant increase in *bax* mRNA expression was also detected from 12 to 24 h (Fig. 6). The expression of *p21* mRNA showed a significantly higher level at 3 h (Fig. 6), and that of *mdm2* mRNA was significantly increased at 12 h (Fig. 6).

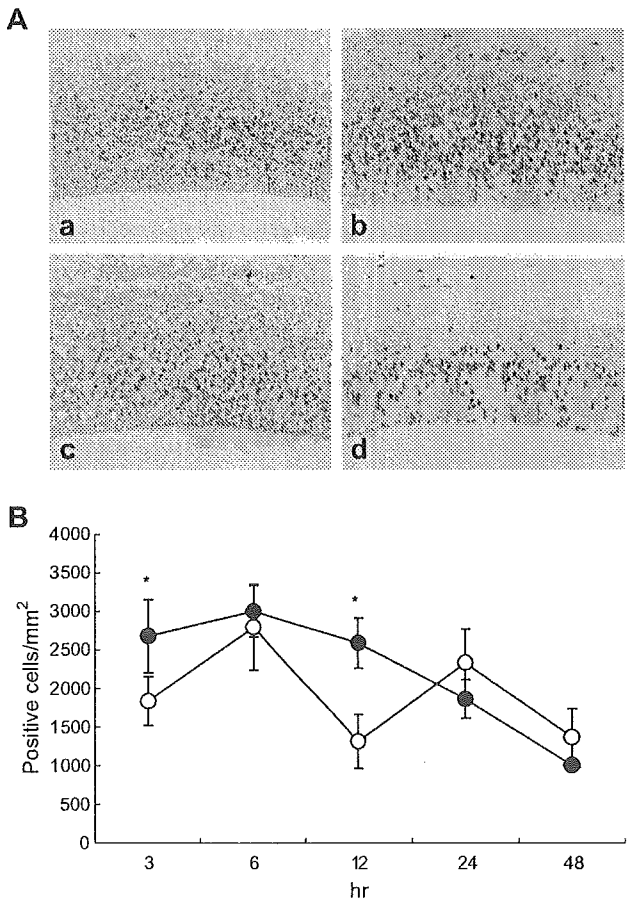

Fig. 4. Immunohistochemical staining for BrdU. (A) BrdU-positive cells in telencephalons of fetuses of the HU-treated group at 3 (a), 6 (b) and 12 h (c), and of a fetus of the control group at 6 h (d). BrdU-positive cells were mainly observed in the middle layer of the ventricular zone at all time point. ×300. (B) Changes in the number of BrdU-positive cells in the fetal telencephalon in the HU-treated (○) and control groups (●). The number of BrdU-positive cells in HU-treated group was not different from that in control group at 6 h. Each value represents the mean±SD for 5 dams. See the note in Fig. 1B.

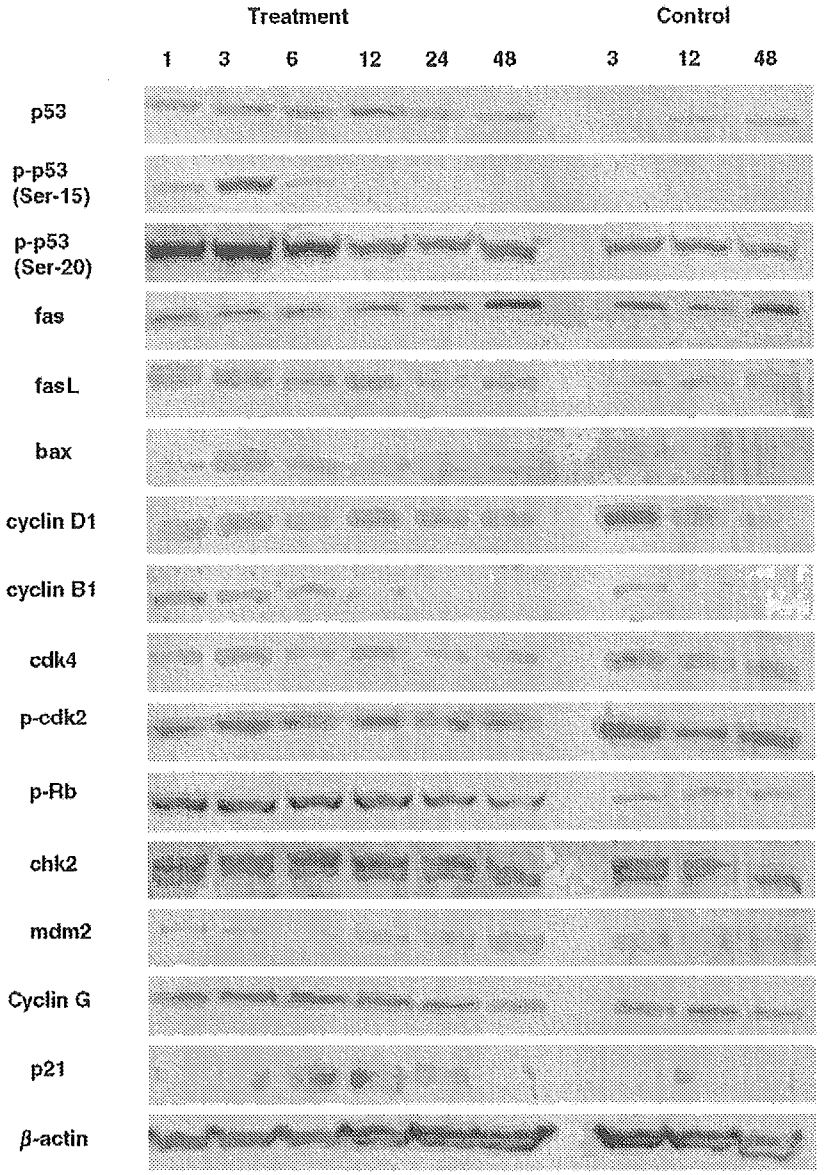

Fig. 5. Western blot analysis of the fetal telencephalon.

No significant changes were observed in the expression of *p53*, *apaf1*, and *cyclin G* mRNAs.

3.4. Flow cytometric anaysis

Flow cytometric analysis demonstrated a time-dependent appearance of DNA debris in the sub-G0/G1 region. The results corresponded well to those for pyknotic cells and TUNEL-positive cells. In addition, exposure to HU resulted in a significant and specific accumulation of cells in the S compartment and G2/M compartment of the cell cycle from 3 to 6 h and at 12 h, respectively (Fig. 7).

Fig. 8A shows the sequential changes in the number of BrdU-positive cells in the control fetal telencephalon. Most neuroepithelial cells entered the S phase after 1 h, moved to the M phase after 6 h, and returned to the G1 phase after 12 h. The results of flow cytometric analysis in the HU-treated group (Fig. 8B) were similar to those for pyknotic cells, TUNEL-positive cells, and BrdU-positive cells.

4. Discussion

It is generally recognized that HU-induced teratogenecity is due to an inhibition of DNA synthesis, which is caused by the blocking of the enzyme ribonucleotide reductase, resulting in a depletion of deoxyribonucleoside triphosphate pools [3,7]. We reported that embryonic maldevelopment was preceded by excessive apoptosis in embryonic target organs when pregnant mice were administrated with HU on day 13 of gestation [39]. In addition, in a study on the neonates and offspring from pregnant mice treated with 400 mg/kg or 800 mg/kg of HU on day 13 of gestation, we reported that the neonates and offspring from pregnant mice treated with HU were retarded in growth, and the organ weights of brain and lungs of the HU-treated

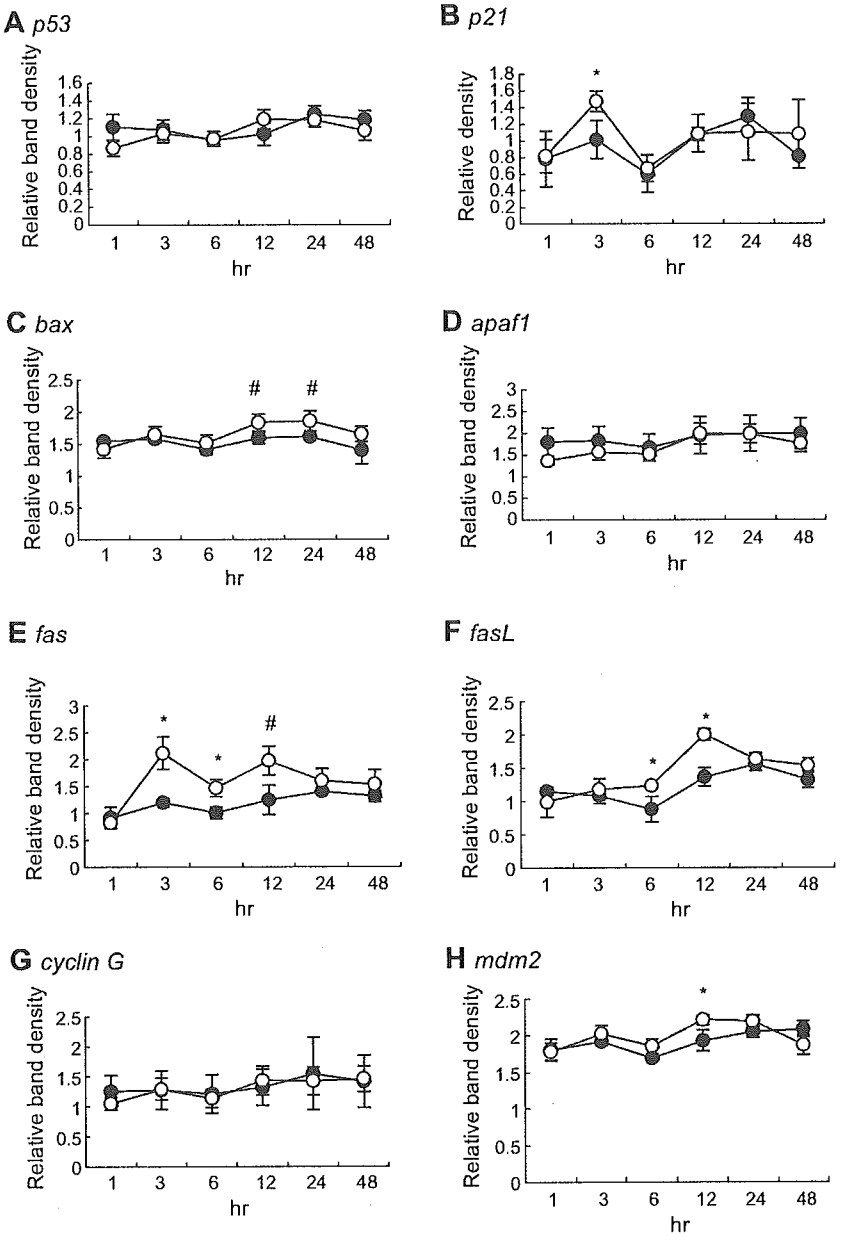

Fig. 6. RT-PCR analysis of sequential changes in the mRNA levels of p53 and its transcriptional targets. Each value represents the mean±SE for 5 dams (HU-treated group) (○) or 3 dams (control group) (●). *$p<0.05$ (Student's t-test), $^{\#}p<0.05$ (Welch's t-test); Significantly different from the control.

group were significantly lower than those of the control group [40].

In the present study, the sequential changes in the expression of p53 and its transcriptional targets (*p21*, *apaf-1*, *bax*, *cyclin G*, *mdm2*, and *fas*) were examined in the fetal mouse telencephalon from dams treated with HU, because p53 is said to play an important role in the induction of apoptosis [20]. Activation of p53 in response to cytotoxic stress such as ionizing radiation [16], glutamate [36] and ischemia [6] depends to a large extent on the stabilization of p53 protein, which rapidly accumulates in stressed cells. Lots of p53-positive neuroepithelial cells were observed from 1 h in the present study, and p53 protein was strongly expressed from 1 h to 12 h. The results indicated that HU-induced apoptosis in the fetal brain was p53-dependent. Also, increases in 53 protein phosphorylated at Serine 15 and 20 were strongly detected from 1 to 6 h. Recent studies have shown that some DNA-damaging agents induce site-specific phosphorylation within the N terminus of p53, specifically at Serine 15, 20, 33, 37, and 46 [1,4,5,29,31,32]. However, no change in *p53* mRNA expression was seen in the present study. In this regard, it is reported that, although the level of *p53* mRNA does not change detectably in response to DNA damage, the level of p53 protein increases rapidly [17].

Degradation of p53 is regulated by interaction with mdm2 protein, which is itself transcriptionally regulated by p53, establishing a negative feedback loop where increased levels of p53 increase the expression of mdm2 [2,12,19]. In the

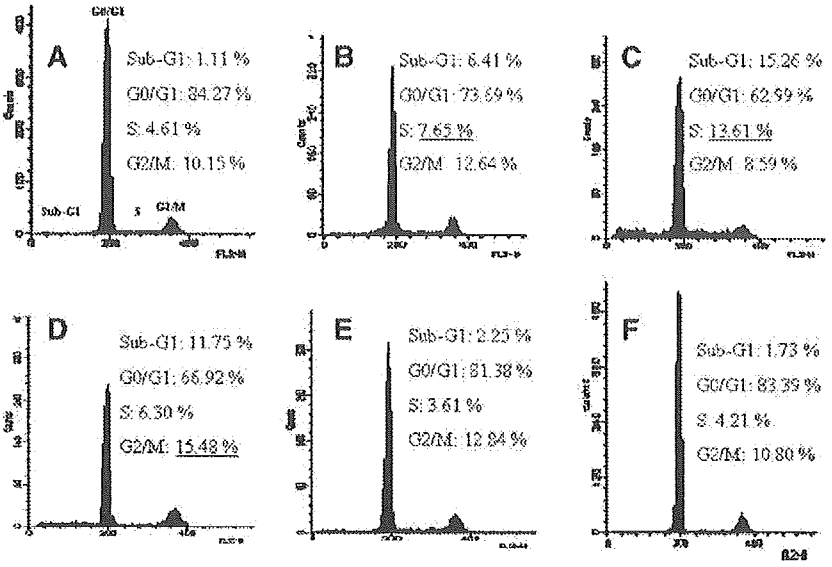

Fig. 7. Cell cycle profile in the neuroepithelial cells of fetal telencephalon at 1 (A), 3 (B), 6 (C), 12 (D) and 24 h (E) after treatment with HU, and of the control group (F). The gates for the sub-G0/G1, G0/G1, S, and G2/M phases are shown.

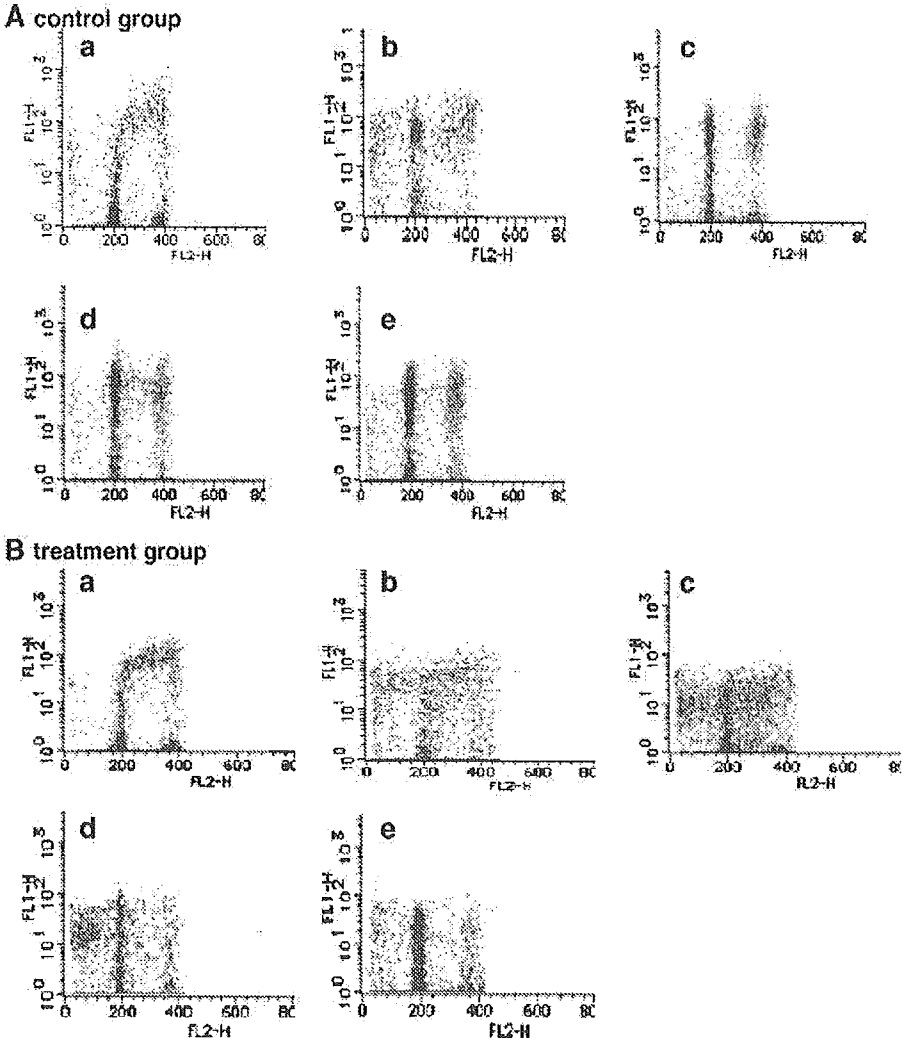

Fig. 8. Flow cytometric analysis of cellular DNA content and BrdU incorporation. (A) BrdU-positive cells in the telencephalon in the control group at 1 (a), 3 (b), 6 (c), 12 (d) and 24 h (e). (B) BrdU-positive cells in the telencephalon in the HU-treated group at 1 (a), 3 (b), 6 (c), 12 (d) and 24 h (e).

present study, the expression of p53 protein gradually increased from 1 to 12 h, and p53 phosphorylated at serines 15 and 20 disappeared or its level was reduced from 12 h. On the other hand, mdm2 protein began to increase at 12 h. Phosphorylation at serines 15 and 37 or at serine 20 was said to reduce the interaction between p53 and mdm2 in vitro [30,38].

p53-induced apoptosis is proposed to be mediated by the transactivation of bax [21], fas/APO1 [24] and p53-inducible genes [25]. Although the timing of the expression of bax protein was not consistent with that of *bax* mRNA, a significant change of bax protein and the mRNA expression was seen in the present study. Early cell changes that occur during apoptosis are associated with mitochondrial changes mediated by the bcl-2 families of proteins, including anti-apoptotic bcl-2 and pro-apoptotic bax proteins [35]. Bax expression is upregulated during p53-dependent apoptosis[21]. Bax accelerates the release of the apoptosis-inducing factor and cytochrome *c* from the mitochondria, thus activating the caspase cascade [33]. In addition, caspase activation was identified by immunochemistry for cleaved caspase 3.

Significant changes in the expression of *fas* and *fasL* mRNAs as well as their proteins were observed in the present study. This suggests an important role for the fas/CD95-fasL receptor-ligand system in HU-induced apoptosis. Fas is induced by p53 in response to genotoxic damaging agents and it is said that fas is necessary for T cell-mediated apoptosis after treatment with anticancer drugs [10,33]. Tumor cells expressing wt p53 are more sensitive to drug-induced apoptosis mediated by fas-dependent signals [23].

In the present study, a significant increase in *p21* mRNA expression appeared at 3 h. An elevation of *p21* mRNA expression was observed following p53 protein expression. Also, the number of BrdU-positive cells, i.e. S phase cells, returned to the level found in the control group at 6 h. In addition, the number of mitotic cells in the inner layer of the ventricular layer significantly increased at 12 h. These findings suggest that HU induces cell arrest. In the flow cytometric analysis, cell cycle arrest was detected at the S checkpoint from 3 to 6 h and at the G2/M checkpoint at 12 h, respectively. p21 is largely responsible for p53-dependent G1 arrest in response to radiation [8]. Negative regulation of the G1 phase cyclin/cdk complex (cyclin D1/cdk 4, 6 and cyclin E/cdk2) plays a key role in the G1/S checkpoint. Cdks are negatively regulated by cdk inhibitors such as p21. Induction and activation of p53 lead to transcriptional induction of p21 owing to strong p53 response elements in the p21 gene promoter. Then, p21 binds and inactivates cyclin D1/cdk4, 6 and cyclin E/cdk2 complexes, resulting in hypophosphorylation of RB and cell cycle arrest [35]. G2 arrest is brought about through signaling cascades that converge to inhibit the activation of cdc2 [13]. Recent study shows that p53 and p21 are necessary to maintain G2 arrest following DNA damage [9]. The mechanism of p53-dependent G2 arrest involves an initial inhibition of cyclin B1/cdc2 activation by p21 and a subsequent reduction of cyclin B1 and cdc2 protein levels [9,14].

Cyclin G1 and apaf-1 are among the targets of the transcription factor, p53. Although the function of cyclin G in the p53 pathway has not been elucidated, it has been reported that cyclin G promotes growth [27,34]. Expression of apaf-1 has been shown to be essential for the p53-dependent apoptosis induced by treatment with DNA-damaging agents [28].

In summary, the neuroepithelial cell death induced by HU may be dependent on p53. Therefore, p53 may form an important link between DNA damage by HU and neuroepithelial cell death.

References

[1] S. Banin, L. Moyal, S. Shieh, Y. Taya, C.W. Anderson, L. Chessa, N.I. Smorodinsky, C. Prives, Y. Reiss, Y. Shiloh, Y. Ziv, Enhanced phosphorylation of p53 by ATM in response to DNA damage, Science 281 (1998) 1674–1677.

[2] Y. Barak, T. Juven, R. Haffner, M. Oren, mdm2 expression is induced by wild type p53 activity, EMBO J. 12 (1993) 461–468.

[3] V. Bianchi, E. Pontis, P. Reichard, Changes of deoxyribonucleoside triphosphate pools induced by hydroxyurea and their relation to DNA synthesis, J. Biol. Chem. 261 (1986) 16037–16042.

[4] D. Bulavin, S. Sairo, M.C. Hollander, K. Sakaguchi, C.W. Anderson, E. Appella, A.J. Fornace, Phosphorylation of human p53 by p38 kinase coordinates N-terminal phosphorylation and apoptosis in response to UV radiation, EMBO J. 18 (1999) 6845–6854.

[5] C.E. Canman, D.S. Lim, K.A. Cimprich, Y. Taya, K. Tamai, K. Sakaguchi, E. Appella, M.B. Kastan, J.D. Siliciano, Activation of the ATM kinase by ionizing radiation and phosphorylation of p53, Science 281 (1998) 1677–1679.

[6] Y.H. Chung, C.M. Shin, M.J. Kim, E.Y. Lee, G. Kim, C.I. Cha, Enhanced expression of p53 in reactive astrocytes following transient focal ischemia, Neurol. Res. 24 (2002) 324–328.

[7] A. Collins, D.J. Oates, Hydroxyurea: effects on deoxyribonucleotide pool sizes correlated with effects on DNA repair in mammalian cells, Eur. J. Biochem. 169 (1987) 299–305.

[8] V. Dulic, W.K. Kaufmann, S.J. Wilson, T.D. Tlsty, E. Lees, J.W. Harper, S.J. Elledge, S.I. Reed, P53-dependent inhibition of cyclin-dependent kinase activities in human fibroblasts during radiation-induced G1 arrest, Cell 76 (1994) 1013–1023.

[9] P.M. Flatt, L.J. Tang, C.D. Scatena, S.T. Szak, J.A. Pietenpol, p53 regulation of G(2) checkpoint is retinoblastoma protein dependent, Mol. Cell Biol. 20 (2000) 4210–4223.

[10] C. Friesen, I. Herr, P.H. Krammer, K.M. Debatin, Involvement of the CD95(APO1/Fas) receptor/ligand system in drug-induced apoptosis in leukemia cells, Nat. Med. 2 (1996) 574–577.

[11] Y. Gravieli, Y. Sherman, S. Ben, Identification programmed cell death in situ via specific labeling of nuclear DNA fragmentation, J. Cell Biol. 119 (1992) 493–501.

[12] Y. Haupt, R. Maya, A. Kazaz, M. Oren, Mdm2 promotes the rapid degradation of p53, Nature 387 (1997) 296–299.

[13] A. Hwang, R.J. Muschel, Radiation and the G2 phase of the cell cycle, Radiat. Res. 150 (1998) S52–S59.

[14] S.A. Innocente, J.L. Abrahamson, J.P. Cogswell, J.M. Lee, p53 regulates a G2 checkpoint through cyclin B1, Proc. Natl. Acad. Sci. U. S. A. 96 (1999) 2147–2152.

[15] M.D. Jacobson, M. Weil, M.C. Raff, Programmed cell death in animal development, Cell 88 (1997) 347–354.

[16] J. Jordan, M.F. Galindo, J.H. Prehn, R.R. Weichselbaum, M. Beckett, G.D. Ghadge, R.P. Roos, J.M. Leiden, R.J. Miller, p53 expression induces apoptosis in hippocampal pyramidal neuron cultures, J. Neurosci. 17 (1997) 397–405.

[17] M.B. Kastan, O. Onyekwere, D. Sidransky, B. Vogelstein, R.W. Craig, Participation of p53 in the cellular response to DNA damage, Cancer Res. 51 (1991) 6304–6311.

[18] K. Katayama, K. Uetsuka, N. Ishigami, H. Nakayama, K. Doi, Apoptotic cell death and cell proliferative activity in the rat fetal central nervous system from dams administered Ethylnitrosourea(ENU), Histol. Histopathol. 16 (2001) 79–85.
[19] M.H.G. Kubbutat, S.N. Jones, K.H. Vousden, Regulation of p53 stability by Mdm2, Nature 387 (1997) 299–303.
[20] N.D. Lakin, S.P. Jackson, Regulation of p53 in response to DNA damage, Oncogene 18 (1999) 7644–7655.
[21] T. Miyashita, J.C. Reed, Tumor suppressor p53 is a direct transcriptional activator of the human bax gene, Cell 80 (1995) 293–299.
[22] J. Morrison, H.J. Wenzel, Y. Kinoshita, C.A. Robbins, L.A. Donehower, P.A. Schwartzkroin, Loss of the p53 tumor suppressor gene protects neurons from kainate-induced cell death, J. Neurosci. 16 (1996) 1337–1345.
[23] M. Muller, S. Strand, H. Hug, E.M. Heinemann, H. Walczak, W.J. Hofmann, W. Stremmel, P.H. Krammer, P.R. Galle, Drug-induced apotosis in hepatoma cells is mediated by the CD95(APO-1/Fas) receptor/ligand system and involves activation of wild-type p53, J. Clin. Invest. 99 (1997) 403–413.
[24] L.B. Owen-Scaub, W. Zhang, J.C. Cusack, L.S. Angelo, S.M. Santee, T. Fujiwara, J.A. Roth, A.B. Deisseroth, W.W. Zhang, E. Kruzel, R. Radinsky, Wild-type human p53 and a temperature-sensitive mutant induce Fas/APO-1 expression, Mol. Cell. Biol. 15 (1995) 3032–3040.
[25] K. Polyak, Y. Xia, J.L. Zweier, K.W. Kinzler, B. Vogelstein, A model for p53-induced apoptosis, Nature 389 (1997) 300–305.
[26] J. Prives, P.A. Hall, The p53 pathway, J. Pahol. 187 (1999) 112–126.
[27] C.L. Reimer, A.M. Boras, S.K. Kurdistanni, J.R. Garreau, M. Chung, S.A. Aaronson, S.W. Lee, Altered regulation of cyclin G in human breast cancer and its specific localization at replication foci in response to DNA damage in p53+/+cells, J. Biol. Chem. 274 (1999) 11022–11029.
[28] A.I. Robles, N.A. Bemmels, A.B. Foraker, C.C. Harris, A PAF-1 is a transcriptional target of p53 in DNA damage-induced apoptosis, Cancer Res. 61 (2001) 6660–6664.
[29] K. Sakaguchi, J.E. Herrera, S. Saito, T. Miki, M. Bustin, A. Vassilev, C.W. Anderson, E. Appella, DNA damage activates p53 through a phosphorylation-acetylation cascade, Genes Dev. 12 (1998) 2831–2841.
[30] S.Y. Shieh, M. Ikeda, Y. Taya, C. Prives, DNA damage-induced phosphorylation of p53 alleviates inhibition by MDM2, Cell 91 (1997) 325–334.
[31] S.Y. Shieh, Y. Taya, C. Prives, DNA damage-inducible phosphorylation of p53 at N-terminal sites including a novel site, Ser20, requires tetramerization, EMBO J. 18 (1999) 1815–1823.
[32] J.D. Siliciano, C.E. Canman, Y. Taya, K. Sakaguchi, E. Appella, M.B. Kastan, DNA damage induces phosphorylation of the amino terminus of p53, Genes Dev. 11 (1997) 3471–3481.
[33] R.V. Sionov, Y. Haupt, The cellular response to p53: the decision between life and death, Oncogene 18 (1999) 6145–6157.
[34] M.L. Smith, H.U. Kontny, R. Bortnick, A.J. Fornace Jr., The p53-regulated cyclin G gene promotes cell growth:p53 downstream effectors cyclin G and Gadd45 exert different effects on cisplatin chemosensitivity, Exp. Cell Res. 230 (1997) 61–68.
[35] Z.A. Stewart, J.A. Pietenpol, p53 signaling and cell cycle checkpoints, Chem. Res. Toxicol. 14 (2001) 243–263.
[36] D. Uberti, M. Belloni, M. Grilli, P. Spano, M. Memo, Induction of tumour-suppressor phosphoprotein p53 in the apoptosis of cultured rat cerebellar neurones triggered by excitatory amino acids, Eur. J. Neurosci. 10 (1998) 246–254.
[37] M. Ueno, K. Katayama, H. Nakayama, K. Doi, Mechanisms of 5-azacytidine(5AzC)-induced toxicity in the rat foetal brain, Int. J. Exp. Pathol. 83 (2002) 139–150.
[38] T. Unger, T. Juven-Gershon, E. Moallem, M. Berger, R. Vogt Sionov, G. Lozano, M. Oren, Y. Haupt, Critical role for Ser20 of human p53 in the negative regulation of p53 by Mdm2, EMBO J. 18 (1999) 1805–1814.
[39] G.H. Woo, K. Katayama, J.Y. Jung, K. Uetsuka, E.J. Bak, H. Nakayama, K. Doi, Hydroxyurea(HU)-induced apoptosis in the mouse fetal tissues, Histol. Histopathol. 18 (2003) 387–392.
[40] G.H. Woo, K. Katayama, E.J. Bak, M. Ueno, H. Yamauchi, K. Uetsuka, H. Nakayama, K. Doi, Effects of prenatal hydroxyurea-treatment on mouse offspring, Exp. Toxic. Pathol. 56 (2004) 1–7.
[41] J.W. Yarbro, Mechanism of action of hydroxyurea, Semin. Oncol. 19 (1992) 1–10.

Available online at www.sciencedirect.com

SCIENCE DIRECT

Experimental and Molecular Pathology 78 (2005) 150–155

Experimental and Molecular Pathology

www.elsevier.com/locate/yexmp

Induction of cytochrome P450 isozymes by phenobarbital in pregnant rat and fetal livers and placenta

Noriko Ejiri, Kei-ichi Katayama, Kunio Doi*

Department of Veterinary Pathology, Graduate School of Agricultural and Life Sciences, The University of Tokyo, Tokyo 113-8657, Japan

Received 20 May 2004, and in revised form 1 July 2004
Available online 15 September 2004

Abstract

Cytochrome P450 (CYP) isozymes are important in metabolizing xenobiotics. They are found in extrahepatic tissues such as placenta as well as liver. Previously, we reported that CYP3A1 was detected in the cytoplasm of giant cells in the trophoblastic region of placenta of rats through pregnancy. In this study, we examined the changes in the expression of CYP proteins in the pregnant rat and fetal livers and placenta after treatment with phenobarbital (PB), one of the antiepileptic drugs which is well known to induce several phase I and phase II drug metabolizing enzymes in the liver. Namely, F344 pregnant rats were treated with PB (80 mg/kg, i.p.) from 13 days of gestation (DG) to 16 DG. All animals were sacrificed on 17 DG, and Western blot analysis and immunohistochemical staining on nine CYP proteins (CYP1A1, CYP2B1, CYP2C6, CYP2C12, CYP2D1, CYP2D4, CYP2E1, CYP3A1, and CYP4A1) and histological examination were done in the dam's liver, placenta, and the fetal liver. Western blot analysis revealed that CYP3A1 protein was significantly induced, CYP2B1 protein was detected, and CYP2D1 protein was significantly decreased in the dam's liver after PB-treatment. In placenta, only CYP3A1 was detected with no difference between control and PB-treated animals. The results of immunohistochemical staining corresponded closely to those of Western blot analysis in the dam's liver and placenta. In the fetal liver, CYP3A1 and CYP2C6 proteins were significantly induced after the PB-treatment, but their immunostainability was not prominent. The present results are considered useful as a basis for further investigation of drug metabolism in pregnant animals.

Keywords: CYP isozymes proteins; Dam's liver; Fetal liver; Placenta; Phenobarbital

Introduction

Cytochrome P450 isozymes (CYPs) are very important in metabolizing xenobiotics. CYPs are divided into several groups by amino acid sequence, and foreign chemicals are metabolized mainly by families CYP 1–4 (Nelson et al., 1993). The majority of CYPs are found in the liver, and some CYPs are found in extrahepatic tissues such as kidneys, adrenal glands, lungs, small intestines, brain, skin, and placenta (Black and Coon, 1987; Simmons and Kasper, 1989).

Although its enzyme files are restricted, placenta is thought to be able to metabolize many foreign chemical compounds. Throughout pregnancy, placenta plays a vital role in maintenance of pregnancy because it has many important endocrine and metabolic functions (Hakkola et al., 1996a; Juchau, 1980).

Previously, we examined the expression of CYP proteins in rat placenta, and reported that CYP3A1 was detected in the cytoplasm of trophoblastic giant cells throughout pregnancy (Ejiri et al., 2001). We examined the induction of CYP3A1 in pregnant rat and fetal livers and placenta, and reported that CYP3A1 was prominently induced by pregnenolone-16α-carbonitrile (PCN) and dexamethasone (DEX) in pregnant rat and fetal livers, but with no significant induction in placenta (Ejiri et al., 2003).

Phenobarbital (PB), an antiepileptic drug, is known to induce several phase I and phase II drug-metabolizing

* Corresponding author. Department of Veterinary Pathology, Graduate School of Agricultural and Life Sciences, The University of Tokyo, 1-1-1 Yayoi, Bunkyo-ku, Tokyo 113-8657, Japan. Fax: +81 3 5841 8185.
E-mail address: akunio@mail.ecc.u-tokyo.ac.jp (K. Doi).

0014-4800/$ - see front matter © 2004 Elsevier Inc. All rights reserved.
doi:10.1016/j.yexmp.2004.07.002

enzymes, especially CYP2B and CYP3A (Asoh et al., 1999). PB administered to pregnant women may exert a variety of effects on the fetus and could contribute to malformations, low birth weight, and so on (Asoh et al., 1999; Bittigau et al., 2003; Gupta and Yaffe, 1982; Holmes et al., 2001). It is said that many chemicals including PB pass through the placenta to the developing fetuses and are rapidly distributed to fetal tissues (Hansen et al., 1999; Papich and Davis, 1986; Welsh, 1982).

This study examines changes in the expression of CYP proteins in pregnant rat and fetal livers and placenta following PB treatment.

Materials and methods

Animals

Ten pregnant rats of the Fischer 344 (F344) strain were purchased from Saitama Experimental Animal Co. (Saitama, Japan). The animals were individually housed in plastic cages in an animal room under controlled conditions (temperature: 23 ± 2 °C; relative humidity 55 ± 5%; light/dark cycle: 14/10 h), and fed commercial pellets (MF, Oriental Yeast Co., Ltd., Tokyo, Japan) and water ad libitum. The day of a vaginal plug being recognized was designated as 0 day of gestation (0 DG).

Chemicals

Phenobarbital sodium (PB) was purchased from Wako Pure Chemical Industries, Ltd. (Tokyo, Japan). PB was dissolved in physiological saline immediately before use, and the concentration was adjusted to 80 mg/ml.

Treatments

From 13 to 16 DG, five dams were daily treated with 80 mg/kg of PB (PB-treated group) intraperitoneally (i.p.) and the remaining 5 dams with 0.1 ml/kg of saline i.p. (control group), respectively.

All animals were sacrificed by exsanguination under ether anesthesia at 17 DG. At necropsy, body weights of dams and fetuses, and liver weight of dams were recorded. Then, the livers of dams and fetuses and placentas were sampled, and half were stored at −80 °C until used for Western blot analysis. The remaining half were fixed in 10% neutral-buffered formalin for histological and immunohistochemical examination.

Western blot analysis

The samples were homogenized with 0.1 M phosphate buffer (PB)–0.15 M KCl–1 mM EDTA Na–1 mM DTT (pH 7.4). The homogenates were centrifuged at 9000 × *g* for 20 min, and then the supernatants were centrifuged at 105,000 × *g* for 60 min. After discarding the supernatant, the pellets were suspended with the same buffer and recentrifuged. The pellets were resuspended with 0.1 M PB–0.15 M KCl–20% glycerol–1 mM EDTA Na–1 mM DTT (pH 7.4), and stored at −80 °C until used. After proteins (10 or 20 μg of mother liver, 30 μg of fetal liver, and 40 μg of placenta) were separated by sodium dodecyl sulfate (SDS)-polyacrylamide gel electrophoresis and transferred to polyvinylidene difluoride (PVDF) membranes. The membrane was treated with anti-rat CYP antibodies. The anti-rat CYP antibodies used in this study were as follows: CYP1A1, CYP2C6, CYP2E1 and CYP4A1 (Daiichi Pure Chemicals Co., Ltd, Tokyo, Japan), and CYP2B1, CYP2C12, CYP3A1, CYP2D1 and CYP2D4 (Chemicon International INC. Temecula, CA). The optimal working dilution was determined based on the results of preliminary examinations. As to the second antibody, anti-rabbit IgG, peroxidase-linked species-specific whole antibody (Amersham Pharmacia Biotech UK Limited, England) (optimal dilution, 1:10,000) and anti-goat IgG, peroxidase-linked species-specific whole antibody (optimal dilution, 1:10,000) were used. ECL Plus system (Amersham Pharmacia Biotech Ltd.) was used to visualize the band, and Quantity One v3.0 (PDI, Inc, NY, USA) was used to quantitate the reactive proteins.

Histology and immunohistochemistry

Paraffin sections (4 μm) were stained with hematoxylin and eosin (HE) for histological examinations. For immunohistochemical examinations, paraffin sections were stained by LSAB method with streptavidine. The above-mentioned antibodies were used as the primary antibody and its optimal working dilutions were determined based on the results of preliminary examinations. The sections were visualized by peroxidase-diaminobenzidine (DAB) reaction, and then counterstained with methyl green.

Statistical analysis

Body weight gain ((body weight at sacrifice − body weight at the beginning of treatment) / body weight at the beginning of treatment × 100) of dams, body weight of fetuses, and relative liver weight of dams (liver weight / body weight × 100) were expressed as mean ± standard deviation (SD) of five dams. Statistical analysis was by the unpaired t-test between the PB-treated and control groups.

Results

Body weights and relative liver weights

No deaths occurred to dams, and there was no difference in fetal mortality between the PB-treated and control groups. The body weight gain of dams and the body weight of fetuses tended to be depressed in the PB-treated group, although not